MINISTRY OF EDUCATION

THE ANNALS OF "DUNAREA DE JOS" UNIVERSITY OF GALATI

Fascicle IX
METALLURGY AND MATERIALS SCIENCE

YEAR XLII (XLVII)
June 2024, no. 2

ISSN 2668-4748; e-ISSN 2668-4756

GALATI UNIVERSITY PRESS
2024

EDITORIAL BOARD

THE ANNALS OF "DUNAREA DE JOS" UNIVERSITY OF GALATI
FASCICLE IX. METALLURGY AND MATERIALS SCIENCE
Nº. 2 - 2024, ISSN 2668-4748; e-ISSN 2668-4756
Volume DOI: https://doi.org/10.35219/mms.2024.2

Table of Contents

THE ANNALS OF "DUNAREA DE JOS" UNIVERSITY OF GALATI
FASCICLE IX. METALLURGY AND MATERIALS SCIENCE
Nº. 2 - 2024, ISSN 2668-4748; e-ISSN 2668-4756
Volume DOI: https://doi.org/10.35219/mms.2024.2

THE ANNALS OF "DUNAREA DE JOS" UNIVERSITY OF GALATI
FASCICLE IX. METALLURGY AND MATERIALS SCIENCE
N°. 2 - 2024, ISSN 2668-4748; e-ISSN 2668-4756
Article DOI: https://doi.org/10.35219/mms.2024.2.01

EXPERIMENTAL RESEARCH ON MODIFICATION OF MECHANICAL PROPERTIES VALUES FOR HEAT TREATED WELDED JOINTS

Marian-Iulian NEACȘU
"Dunarea de Jos" University of Galati, Romania
e-mail: mneacsu@ugal.ro

ABSTRACT

This paper presents the results of studies and research on the values of the mechanical properties of welded joints on OLC 20 and OLC 25 steel samples, in the case that no heat treatment is performed on them and in several cases when the samples are heat treated after welding. After welding and heat treatments for normalization, hardening and tempering was carried out on the samples.

After performing the heat treatments, the researched samples were subjected to tests to determine: Vickers hardness, mechanical resistance Rm and breaking energy KV.

Analysing the obtained results, it can be concluded that following the thermal normalization treatment, the optimal complex of the values of the studied mechanical properties was obtained.

KEYWORDS: welding, heat treatment, hardness, mechanical resistance, breaking energy

1. Introduction

The superior valorisation of metallic materials imposes special qualitative tasks in the entire industrial and scientific metallurgical activity currently oriented towards the adoption of those modern technologies that allow the reduction of metal consumption, the increase of the durability and performance of the highly technical products specified to be realized in the construction of machines, aeronautics, electronics and energy.

Countries with highly developed economies leave their mark on the global economy and try to consolidate their position in a very dynamic and highly competitive market. This desire can only be achieved by permanently investing in research and by streamlining industrial production, which holds the majority of the country's gross income. An important role in this competition is also the training of specialists, who can contribute directly to the increase in the quality of products, in conditions of economic efficiency. Thus, it follows the importance of evaluating the economic contribution and the impact on the productivity of welding materials, in the industrial branches where welding is a key element in the manufacturing process. If there is still some scepticism about this, we can mention that in the US, durable industrial goods where welding is a critical component in the manufacturing process, these goods represent 90% of all manufactured industrial goods [1, 2].

According to the same report, the industrial branches in which the welding of materials is a key element in the manufacturing process represent 59 % of the total industrial production [1].

Increasing the degree of complexity and product typification actions, optimizing the activity of choosing or assimilating new brands of alloys involves a process of qualitative renewal of both domestic metal production and scientific thinking in the field of elaboration and processing of metallic materials [3].

Over 70 % of the total welding expenses are held by labour expenses. In this context, it is easy to understand that these industrial fields, dominated by welding technologies, have a major contribution to the gross domestic product (GDP) of industrially developed countries and are strategic sectors that ensure a positive trade balance. The interest given to improving the global competitiveness of these industries with a major impact on the economy is obvious, this being achieved mainly by increasing the performance and profitability of companies, which are based on welding technologies [4].

THE ANNALS OF "DUNAREA DE JOS" UNIVERSITY OF GALATI
FASCICLE IX. METALLURGY AND MATERIALS SCIENCE
Nº. 2 - 2024, ISSN 2668-4748; e-ISSN 2668-4756
Article DOI: https://doi.org/10.35219/mms.2024.2.01

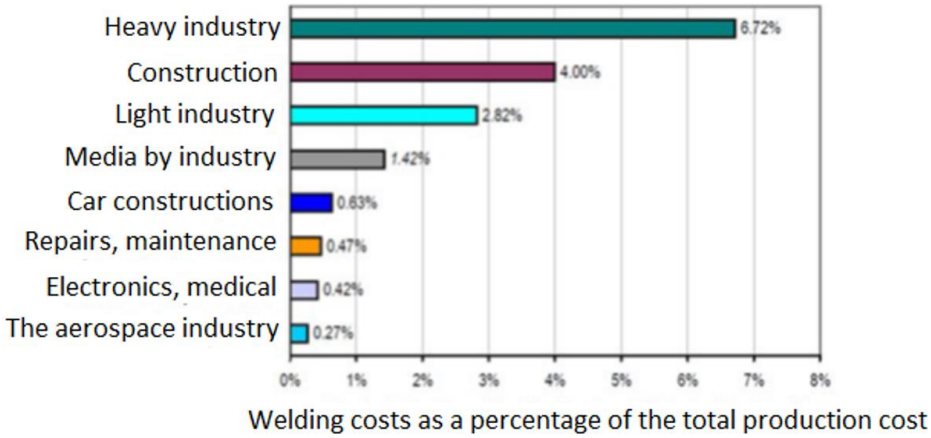

Fig. 1. *The share of welding costs from the total production costs* [1]

The properties imposed on steel products intended for the realization of various metal constructions undergo changes, more or less important, as a result of the subsequent processing to which they are subjected. Steels undergo the greatest changes due to the action of welding thermal cycles as a result of rapid heating during welding and the thermal conductivity of the base metal, hard constituents with reduced ductility appear in the affected area. The ability of a heat affected zone and weld bead to respond to heat treatment without compromising the strength of the welded structure is a common area of research for steel and filler manufacturers, designers and builders [5].

The welded joints were executed on the base metal, so the entire welded structure is required to withstand the stresses foreseen in operation. The satisfaction of this condition, however, depends on the welding behavior of the steels, which cannot be guaranteed for all welding processes, depending on both the base metal and the geometry of the joint, the manufacturing conditions and the service regime of the welded assembly. The risk of brittle fracture of welded joints has determined the initiation of extensive research, which resulted in the design of a great diversity of tests and criteria for interpreting the results. However, there are serious difficulties in assessing the reduction in brittle fracture resistance of steels, as a result of the hardening they undergo under the action of the welding process [6].

Steels for constructions and welded structures are those steels that are used in the manufacture by welding of structures that are especially mechanically stressed and operated at temperatures between -50 °C and +50 °C. They must satisfy three fundamental requirements [7, 8]:

- to weld well with relatively simple and high productivity procedures.
- to have as high mechanical characteristics as possible to create light structures;
- to be cheap so as not to make the structure more expensive;

According to the specifics of the operating conditions, the following categories of steel for construction and welded structures appear [9, 10]:

• steels for general use;
• steels for devices and containers under pressure;
• steels for shipbuilding and marine platforms.

The separation between these groups results from the differences in operating characteristics and quality control rules.

The problem of the choice of filler materials is generally complex and considers ensuring in the weld some strength characteristics at least equal to those of the base metal and a chemical homogeneity acceptable from a functional and economic point of view.

Apart from these general criteria, the compatibility between the base metal (MB) and the filler metal (MA) must also be considered. By this, it is meant the property of a filler metal (MA) to couple with a certain steel, under certain welding conditions, to make a welded joint that corresponds to the required technical and functional characteristics. In general, filler materials are produced in the form of electrodes, wires and fluxes for welding [11].

2. Experimental conditions

The experimental material is represented by two samples welded by the manual electric process, the base material consisting of two raw forged and machined plates with a thickness of 20 mm and a length of 500 mm.

The quality of the base material is OLC 20 for the first sample, respectively OLC 25 for the other, the welding being performed with covered electrodes type E 424B42H10 in both cases [11, 12].

THE ANNALS OF "DUNAREA DE JOS" UNIVERSITY OF GALATI
FASCICLE IX. METALLURGY AND MATERIALS SCIENCE
No. 2 - 2024, ISSN 2668-4748; e-ISSN 2668-4756
Article DOI: https://doi.org/10.35219/mms.2024.2.01

The chemical composition and mechanical property values for the base material, in the as-forged state, are shown in table 1 (Chemical composition) and table 2 (Mechanical property values).

Table 1. *Chemical composition of the base material*

	C	Mn	Si	S	P	Cr	Ni	Cu	Al
OLC 20	0.21	0.42	0.26	0.024	0.014	0.21	0.19	0.3	0.026
OLC 25	0.23	0.50	0.28	0.007	0.011	0.19	0.17	0.03	0.031

Table 2. *Values of mechanical properties* [13]

	$Rp_{0,2}$ [MPa]	Rm [MPa]	A [%]	KV [Joule]
OLC 20	277	433	25	30
OLC 25	291	453	23	28

Table 3. *Chemical composition and mechanical characteristics for the filler material* [13]

Chemical composition [%]				
C=0.071	Mn=0.792	Si=0.331	P=0.009	S=0.021
Mechanical tests				
$Rp_{0,2}$ [MPa]	**Rm [MPa]**	**A [%]**	**KV (Joule)**	
471	586	29	214	

Mechanical tests or carried out at room temperature, in accordance with the applicable standards SR EN 10002/1:2002 (tensile test) [14] and SR EN 10045/1:1993 (shock bending test) [15]. The chemical composition and mechanical characteristics for the aggregate material are certified by their manufacturer, as shown in Table 3.

The specification of the welding process used is as follows:

• preheating temperature 120 ± 10 °C;
• temperature between layers 200 ± 15 °C;
• current intensity and arc voltage for the root layer: I1 = 90 ± 5 A;
Ul = 22 ± 1 V;
• current intensity and arc voltage for the filling layer: I2 = 125 ± 5 A;
U2 = 23 ± 1 V.

In many cases, the application of a heat treatment ensures the joining by welding of steels considered non-weldable or difficult to weld without it.

Currently, it is believed that with any properly prepared and processed steel, a welding technology can be established that allows obtaining the operational characteristics required for the welded joint.

Since the welding process involves rapid heating and cooling of the material, it can be compared to the action of a thermal shock. The ability of the material to withstand shock action without degrading defines its weldability. The action of thermal shock can decrease in intensity by applying a certain type of heat treatment.

The following post-weld heat treatments were applied to the investigated steels, OLC 20 and OLC 25: normalizing, and tempering.

In order to improve the metallurgical structure and implicitly the mechanical properties, a thermal normalization treatment was carried out, identical for the two samples:

• heating speed 80 °C/h;
• maintenance temperature 915 °C;
• holding time 30 minutes;
• cooling in still air.

The tempering parameters were as follows:

• heating speed 80 °C/h;
• maintenance temperature 860 °C;
• holding time 15 minutes;
• cooling in oil.

Next, the evolution of the mechanical properties of the joints was followed by applying an annealing heat treatment with the following parameters:

• heating speed 80 °C/h;
• maintenance temperature 360 °C;
• holding time 15 minutes;
• cooling in still air.

3. Results of experimental research

The initial mechanical characteristics of the welded and untreated samples, strength and toughness characteristics were verified. For this, the following tests were performed at room temperature:

a) transverse tensile test, according to SR EN 10002/1:2002 [14];

b) shock bending test, according to SR EN 10045/1:1993 [15];

THE ANNALS OF "DUNAREA DE JOS" UNIVERSITY OF GALATI
FASCICLE IX. METALLURGY AND MATERIALS SCIENCE
N°. 2 - 2024, ISSN 2668-4748; e-ISSN 2668-4756
Article DOI: https://doi.org/10.35219/mms.2024.2.01

c) Vickers hardness test SR EN 1043-1:2004 [16];

d) mandrel bending test, according to SR EN ISO 156/4-1:2004 [17].

Bending on the mandrel was done on a mandrel with a diameter of D = 60 mm, as required in SR EN ISO 156/4-1:2004 which regulates the verification of the electric arc welding process of steels, determining the angle from which on a crack with a length of at least 2 mm is formed on the surface of the test piece.

The shock bending test was performed on sets of three ISO-V specimens, with the notch-oriented perpendicular to the face of the welded plate and centered successively in the base material, the heat-affected zone and the filler material. The positioning of the notch was achieved by attacking with Nital 2% reagents the samples flowed perpendicular to the weld bead and ground on the side faces to a cross section of 10 x 10 mm^2. The breaking energy was determined as the arithmetic mean of the values obtained on the set consisting of three samples from each area of interest.

The variation of the Vickers hardness in the joint section depending on the state of the samples, non-thermally treated or thermally treated, is shown in figure 2, 3 and 4 with the observation that the test load is 10 kgf and the working method is that of SR EN 1043-1:2004.

Comparing the hardness measurement results between untreated and heat-treated welded samples, it is obvious that the most convenient results are for normalized samples, but also the combination of hardening followed by tempering is a solution for improving the mechanical properties of the joint.

In the case of return, the hardness variation when passing from the base material to the heat-affected zone is 47 HV10 compared to 84 HV10 for OLC 20, respectively 60 HV10 compared to 110 HV10 for OLC 25. Although this ratio of approximately 2:1 is reduced sensitively, the variation of hardness when passing from the heat-affected zone to the filler material is less after the improvement treatment compared to the case of the untreated welded samples, 40 HV10 compared to 39 HV10 for OLC 20, respectively 59 HV10 compared to 76 HV10 for OLC 25.

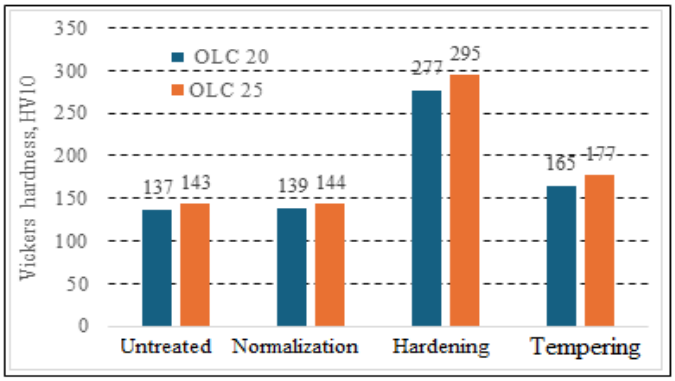

Fig. 2. *Variation of HV hardness in the MB area for the two investigated steel brands depending on the heat treatment applied*

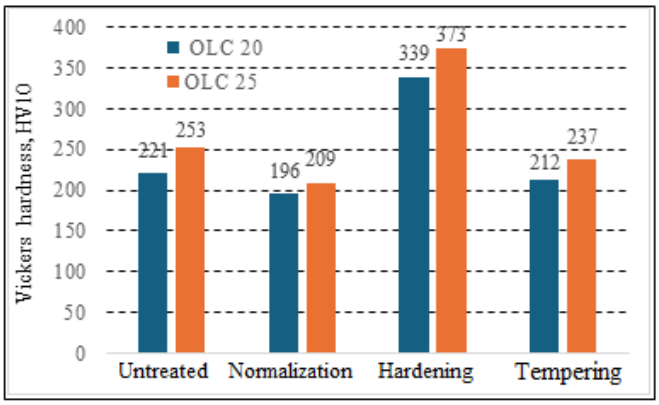

Fig. 3. *Variation of HV hardness in the ZIT zone for the two investigated steel brands depending on the heat treatment applied*

THE ANNALS OF "DUNAREA DE JOS" UNIVERSITY OF GALATI
FASCICLE IX. METALLURGY AND MATERIALS SCIENCE
Nº. 2 - 2024, ISSN 2668-4748; e-ISSN 2668-4756
Article DOI: https://doi.org/10.35219/mms.2024.2.01

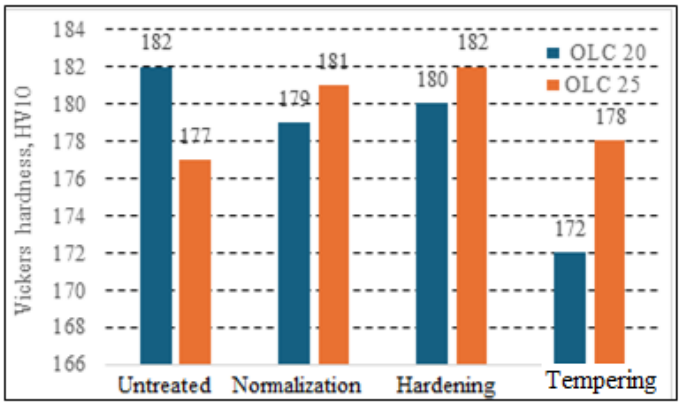

Fig. 4. *Variation of HV hardness in the MA area for the two investigated steel brands depending on the heat treatment applied*

The results of the fracture energy variation for the investigated samples are illustrated in the graphs in Figures 5, 6 and 7.

After analysing the data obtained for the breaking energy, it can be concluded that the values of the breaking energy are higher in the treated samples compared to the untreated samples. Overall, the toughness gain is more important after the normalizing heat treatment compared to the tempering heat treatment.

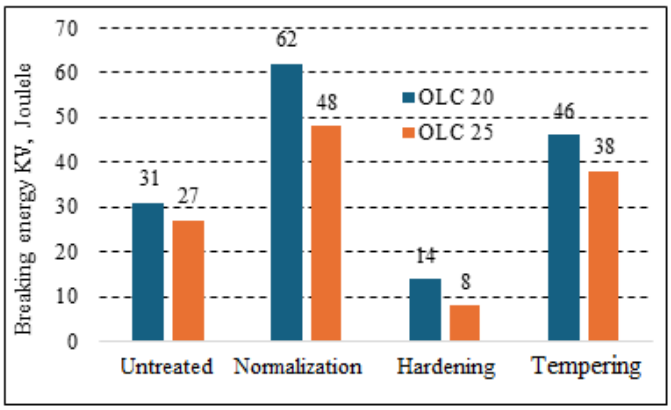

Fig. 5. *Variation of KV in the MB area for the two investigated steel grades depending on the heat treatment applied*

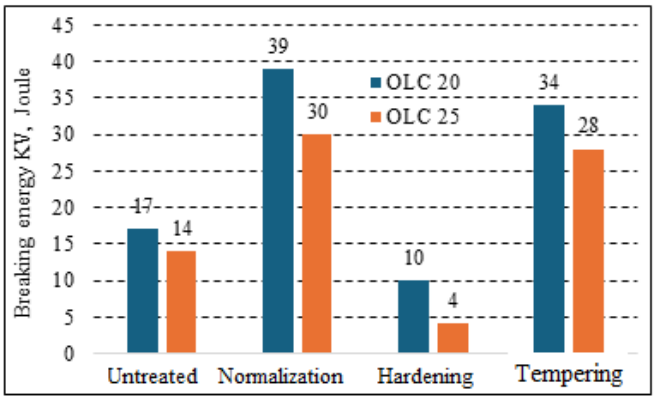

Fig. 6. *Variation of KV in the ZIT area for the two investigated steel brands depending on the heat treatment applied*

THE ANNALS OF "DUNAREA DE JOS" UNIVERSITY OF GALATI
FASCICLE IX. METALLURGY AND MATERIALS SCIENCE
No. 2 - 2024, ISSN 2668-4748; e-ISSN 2668-4756
Article DOI: https://doi.org/10.35219/mms.2024.2.01

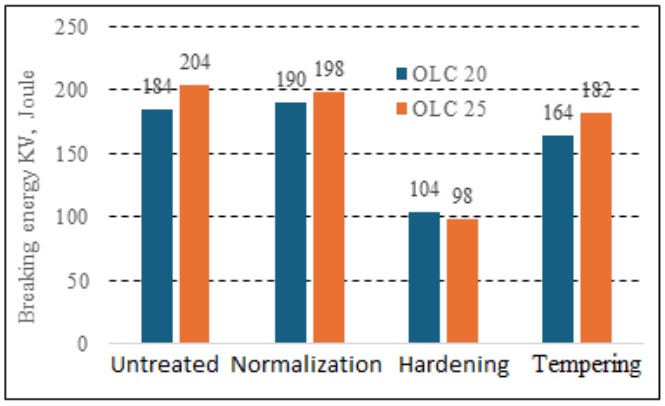

Fig. 7. *Variation of KV in the MA zone for the two investigated steel brands depending on the heat treatment applied*

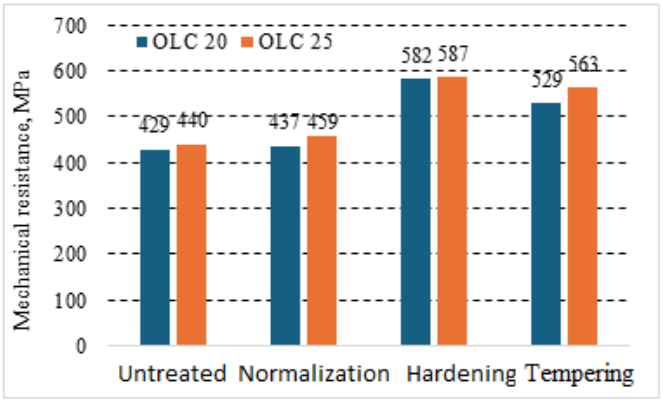

Fig. 8. *Rm variation for the two investigated steel grades depending on the heat treatment applied*

Figure 8 shows the variation in breaking strength depending on the state of the investigated samples (thermally treated or untreated). The highest values of the mechanical strength were obtained for the hardened samples, then for those subjected to the tempering treatment followed by the values of the normalized samples and the lowest values of the resistance were recorded for the non-thermally treated samples.

4. Conclusion

Relating the gain obtained in the improvement of the mechanical properties to the apparent expenses of the thermal treatments applied, it can be concluded that the optimal solution for the studied materials is the normalization thermal treatment, which leads to a satisfactory mechanical resistance, combined with a capacity for plastic deformation and a toughness that can be characterized as very good.

Taking into account the above, the positive influence of heat treatments results from normalization and recovery of the mechanical characteristics of welded joints with OLC 20 / OLC 25 base material.

By comparison with the results obtained after the normalization heat treatment, we find that the welded samples and to which an annealing heat treatment was applied have a superior mechanical strength, the break occurring in the base material at values above 500 MPa in each case. The superiority of the tempering heat treatment consists in obtaining a mechanical resistance to breaking higher by about 100 MPa compared to the normalizing heat treatment.

Under identical welding and heat treatment conditions, it was found that the normalizing heat treatment was superior to the annealing treatment in terms of joint toughness, while the plastic deformation capacity, tested by the mandrel bending test, remained satisfactory.

Comparing the results of the tests and examinations carried out for the two materials, we notice that in the conditions where the chemical composition does not apparently show significant differences, the welding behavior of the OLC 20 material is significantly superior to the OLC 25

material, highlighting the value of the concept of equivalent carbon as a working tool.

References

[1]. ***, *Welding-Related Expenditures, Investments and Productivity Measurement in U.S. Manufacturing*, Construction, and Mining Industries, 2002.
[2]. Bodea Marius, *Sudare şi procedee conexe*, Editura Utpress Cluj-Napoca, ISBN 978-606-737-143-7, 2016.
[3]. Dorin Dehelean, *Sudarea prin topire*, Editura Sudura, Timişoara, 1997.
[4]. Zgură G., Răileanu D., *Tehnologia sudării prin topire*, Editura Didactică şi Pedagogică, Bucureşti, 1983.
[5]. Echim I., Lupescu I., Nicoară L., *Tehnologii pentru sudarea prin topire a oţelurilor*, Editura Tehnică, Bucureşti, 2002.
[6]. Mircea Burcă, Stelian Negoiţescu, *Sudarea MIG-MAG*, Editura Sudura, Timişoara, 2002.
[7]. Tusz Francisc, *Tratat de sudură*, Editura Sudura, Timişoara, 2003.
[8]. Mihăilescu D., Mihăilescu A., Lupu G., *Tehnologia sudării prin topire - Îndrumar de proiectare*, Editura Fundaţiei Universitare Dunărea de Jos, Galaţi, 2004.
[9]. Dorin Şerban, Eugen Găvan, *Tehnologii de asamblare şi sudare a corpului navei*, Editura Evrika, Brăila, 2001.
[10]. Berinde V., Ánghel I., *Sudarea cu arc electric - Ghid pentru autoinstruirea sudorilor*, Editura Tehnică, Bucureşti, 2010.
[11]. ***, *Cărţi tehnice furnizor echipamente sudare Kemppi*, Finlanda, ESAB – Suedia.
[12]. ***, *Instrucţiuni tehnologice SNDG: I.T.*, nr. 2299, 2300, 2303, 2305, 2339, 2356, 2274 A, 2297.
[13]. Mitelea V. Budau, *Materiale și tratamente termice pentru structuri sudate*, Editura de Vest, Timișoara, 1992.
[14]. ***, SR EN 10002/1:2002.
[15]. ***, SR EN 10045/1:1993.
[16]. ***, SR EN 1043-1:2004.
[17]. ***, SR EN ISO 156/4-1:2004.

THE ANNALS OF "DUNAREA DE JOS" UNIVERSITY OF GALATI
FASCICLE IX. METALLURGY AND MATERIALS SCIENCE
N°. 2 - 2024, ISSN 2668-4748; e-ISSN 2668-4756
Article DOI: https://doi.org/10.35219/mms.2024.2.02

THE IMPACT ASSESSMENT OF THE MINERAL AGGREGATES' DEPOSITS ON THE STORAGE AREA

Anca ȘERBAN, Adrian LEOPA
"Dunarea de Jos" University of Galati, Faculty of Engineering and Agronomy in Braila,
Calarasilor Street, 29, RO-810017, Braila, Romania
e-mail: adrian.leopa@ugal.ro

ABSTRACT

The construction sector is vital for our modern society such that most of the modern activities are dependent on constructions. The demographic increase and the longing of our times to better living conditions are the main exponents of unprecedented development in the construction field. The consequence of this phenomenon is the continuous growth of waste from construction and demolition. The management of these waste according to the sustainable development principles involves recycling or where not possible their storage considering the environmental tasks. This paper marks out the management of the two construction and demolition wastes, gas-formed concrete and concrete, taking account of the chemical composition of the leachate resulted from the waste drainage in the ground due to precipitation.

KEYWORDS: construction wastes, storage, soil pollution, leachate

1. Introduction

According to the report "Our common future" (Bruntland Report) issued by the World Commission on Environment and Development (WCEF) the definition of sustainable development is the following: "the sustainable development is the development that aims to meet the needs of the present without compromising the possibilities of future generations to meet their own needs" [1]. In the category "their own needs" the primary resources are also included (most of them), since these are exhaustible, even if up to the present time there have not been discovered all the existing reserves. Thus, we realize that today's generations have the moral obligation not to consume at an accelerated rate (or even run down) the primary resources presently available.

The possibility of a judicious management of primary materials is the use of waste as a secondary raw material. In support of it, the directive 2008/98 CE imposes a waste hierarchy which sets the order of waste management priorities as follows: waste prevention, preparation for reuse, recycling, recovery, and disposal. The protection of primary resources stems from the waste hierarchy as a direct advantage of recycling.

Consequently, the activity designed to protect primary resources, and which is also a principle of sustainable development is the waste recycling.

Regarding the recycling of mineral waste from construction and demolition (CD) both at national and European level, there are legislative norms regulating this domain.

At European level the Directive 2008/98 CE imposes that "by 2020, the preparing for re-use, recycling and other material recovery, including backfilling operations using waste to substitute other materials, of non-hazardous construction and demolition waste excluding naturally occurring material defined in category 17 05 04 in the list of waste shall be increased to a minimum of 70 % by weight".

Another important step in this direction is the EU Protocol on Building and Demolition Waste Management (EU Construction and Demolition Waste Protocol) (concluded in November 2016) which aims to increase the confidence in the CD waste management process as well as in the quality of waste generated by this field [2]. For this purpose, the structure of the protocol is based on five components, which are as follows:

- identification, source separation and waste collection;
- waste logistics;
- waste treatment;

THE ANNALS OF "DUNAREA DE JOS" UNIVERSITY OF GALATI
FASCICLE IX. METALLURGY AND MATERIALS SCIENCE
N°. 2 - 2024, ISSN 2668-4748; e-ISSN 2668-4756
Article DOI: https://doi.org/10.35219/mms.2024.2.02

- quality management;
- politics and the framework conditions [3].

2. The recycling of CD waste in European countries

In the European Union there is, at least at a legislative level, the optimum framework of a sustainable management of construction and demolition wastes.

At the European Union level, the amount of construction and demolition waste is around 20-30 of the total waste [2]. In a report made in 2008, the Umweltbundesamt (Environmental Federal Agency from Germany) estimates that 200 million tons of CD waste are generated annually at EU level (without considering the excavated soil), that is over 0.5 tons per capita. In the same context, the FEAD estimates for the same indicator a value ranging from 1.5 to 2 tons per capita [2]. According to the experts in the field, the disparities between these reports are due to differences between the definitions and reporting mechanisms as well as uneven levels of control and data reporting [2]. Therefore, a major problem in the management of construction and demolition waste is the exact estimation of the quantities collected.

This problem is also faced by Romania due to the absence of a regulated market for construction and demolition waste, and there are no recent and accurate statistical data on their management. In 2017, at the level of the Ministry of Environment, a legislative act is in the process of being prepared, concerning the management of the waste from construction and demolition waste which has as main objective the transition from a linear economy to a circular one [5].

Another objective of the European Union is the transition from a linear economy to a circular one according to which the waste will no longer be disposed of by incineration or stored but will re-enter into circulation. In this context, at the level of 2012, 5 billion tons of raw materials were consumed at the level of the 28 Member States. 80% of these were from primary resources, and the remaining 20% came from secondary raw materials, which meant a 20% recirculation rate. At the same year, 2.5 billion tons of waste were disposed of, out of which 42% was stored [6].

Even if at national level there is no centralized situation of construction and demolition waste, these waste fractions exist and the evidence of this is the statistical data regarding the construction development in Romania provided by the National Institute of Statistics. Based on these statistical data, the graphs of the monthly progress of the construction developments were represented regarding the construction objects (Figure 1) and the construction elements (Figure 2) related to the period from 2010 to 2018 [7].

Statistical data of the histogram in Figure 2 notes the following aspects:

- the volume of developments at the new constructions exceeds the reference value (year 2015) in 2010, 2011, 2012, 2015, 2016, 2017 and 2018;
- the volume of major repair developments exceeds the reference value (year 2015) only in 2013 and 2015;
- the volume of current repair and maintenance developments exceeds the reference value (year 2015) in 2011, 2013 and 2016.

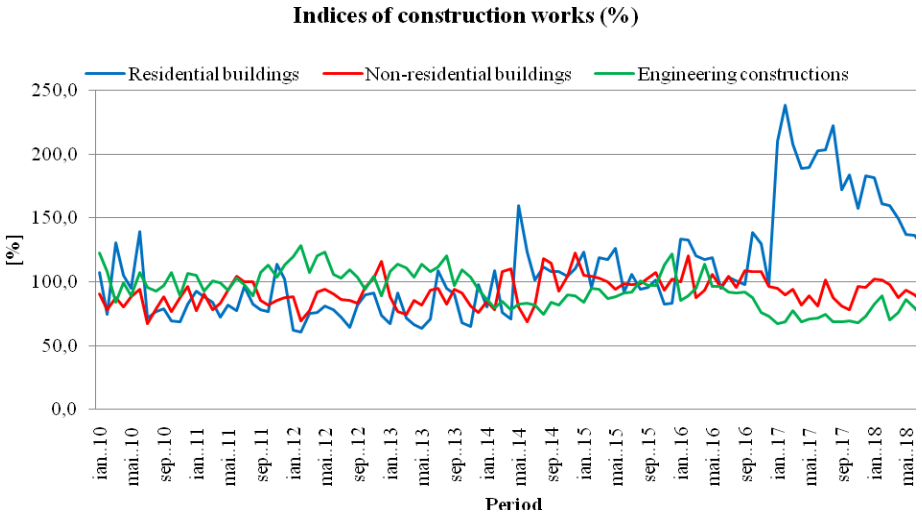

Fig. 1. *Indices of construction development (%) on construction objects; adjusted series according to the number of working days and seasonality. Stated as an index where 2015=100* [7]

THE ANNALS OF "DUNAREA DE JOS" UNIVERSITY OF GALATI
FASCICLE IX. METALLURGY AND MATERIALS SCIENCE
Nº. 2 - 2024, ISSN 2668-4748; e-ISSN 2668-4756
Article DOI: https://doi.org/10.35219/mms.2024.2.02

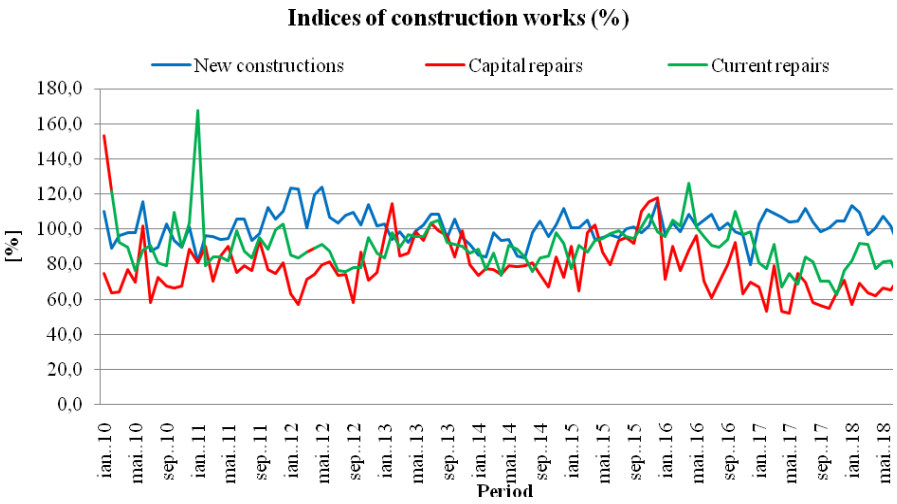

Fig. 2. *Indices of construction development (%) on construction elements; adjusted series according to the number of working days and seasonality. Stated as an index where 2015=100* [7]

The analysis of the two histograms of the evolution of construction development shows that at national level there are activities in the construction field which generate significant quantities of waste. Most of these waste fractions are disposed of in dump sites for inert waste.

3. Results

The humidity of the test materials was very low, namely 0.753 % for AAC and 0.233 % for concrete. The reaction of the eluates was moderately alkaline at the eluate from the two-stage batch leaching test (Table 3) and strongly alkaline at the eluate from one stage batch leaching test (Table 2).

The Total Dissolved Solid Materials is very high in both tests and for both materials, and yet exceeded the limit value at eluate from AAC for L/S = 2+8 L/kg. The high content of minerals is also reflected in the conductivity values, which were higher at the eluates from AAC in both tests.

The values of eluates hardness do not show an important content of calcium and magnesium salts. The calcium ions have higher concentration in the eluates from L/S = 10 L/kg for both test materials, while the magnesium ions are generally low, but recorded the highest value at AAC eluate from L/S = 2+8 L/kg.

The cations content in the eluates refers to the hydrogen carbonates HCO_3^-, chloride Cl^- and sulphate SO_4^{2-}. The hydrogen carbonates have higher values in the eluates from L/S = 10 L/kg for both test materials. The limit value of chloride is not exceeded in both cases of eluates and materials, but the value of eluate from concrete at ratio L/S = 10 L/kg is particularly remarkable. The sulphate ions are present in concentrations exceeding the limit value except for the one from the eluate from concrete at ratio L/S = 2+8 L/kg.

Table 1. *The results of eluates analysis for L/S = 10 L/kg*

Indicator and measure unit	The values for AAC eluate	The values for concrete eluate	Limit values for leachability of inert waste (Ordinance 95/2005)
Conductivity mS/cm	2.305	1.087	-
TDS mg/kg	3290	3055	4000 mg/kg
pH	9.0	11.36	-
Temporary hardness ºd	1.792 ºd	1.456 ºd	-
HCO_3^-, mg/kg	390.4	317.2	-
Cl^-, mg/kg	132,93	453.76	800 mg/kg
SO_4^{2-}, mg/kg	3552	1248	1000 mg/kg
Ca^{2+}, mg/kg	480.09	729.4	-
Mg^{2+}, mg/kg	47.8	27.7	-

THE ANNALS OF "DUNAREA DE JOS" UNIVERSITY OF GALATI
FASCICLE IX. METALLURGY AND MATERIALS SCIENCE
Nº. 2 - 2024, ISSN 2668-4748; e-ISSN 2668-4756
Article DOI: https://doi.org/10.35219/mms.2024.2.02

Table 2. *The results of eluates analysis for L/S = 2+8 L/kg*

Indicator and measure unit	The values for AAC eluate	The values for concrete eluate	Limit values for leachability of inert waste (Ordinance 95/2005)
Conductivity mS/cm	1.874	0.838	-
TDS mg/kg	5200	2140	4000 mg/kg
pH	8.25	8.11	-
Temporary hardness ºd	1.764 ºd	1.372 ºd	-
HCO_3^-, mg/kg	277.69	147.05	-
Cl^-, mg/kg	430.35	369.75	800 mg/kg
SO_4^{2-}, mg/kg	2358.5	708.4	1000 mg/kg
Ca^{2+}, mg/kg	289.6	394.3	-
Mg^{2+}, mg/kg	127.4	12.3	-

4. Materials and Methods

In Romania, the wastes are governed by the Law 211/2011concerning the waste regime and by the HG 856/2002 concerning the waste classification and management.

To be stored and accepted in deposits, the Romanian legislation states that the wastes must meet certain chemical characteristics according to Ordinance 95/2005 The determination of the criteria of acceptance and preliminary procedures for the acceptance of waste from storage and the national list of wastes accepted in each class of waste deposit.

The first leaching test will be performed according to the standard SR EN 12457-2/2003- The waste characterization. Levigating. The conformity assessment test for granular waste and sewage sludge levigating. Part 2: One stage batch leaching test at liquid-solid ratio of 10 L/kg for material with particle size less than 4 mm.

The Romanian Ordinance 95/2005 provides for the leaching tests according to SR EN 12457/1-4:

- Part 1: L/S = 2 L/kg, particle size < 4 mm.
- Part 2: L/S = 10 L/kg, particle size < 4 mm.
- Part 3: L/S = 2 + 8 L/kg, particle size < 4 mm.
- Part 4: L/S = 10 L/kg, particle size < 10 mm.

According to the European legislation, the batch leaching test EN 12457/1-4 consists of 4 parts:

1. EN 12457-1: Performed at L/S 2 L/kg on material < 4 mm (1 step).
2. EN 12457-2: Performed at L/S 10 L/kg on material < 4 mm (1 step).
3. EN 12457-3: Performed at L/S 2 L/kg and L/S 8 L/kg on material < 4 mm (2 steps).
4. EN 12457-4: Performed at L/S 10 L/kg on material < 10 mm (1 step).

The test material 1 was the autoclaved aerated concrete (AAC) and it was part of a construction completed in 1987. The material was not exposed to the elements and was not held in inadequate conditions. The test material 2 was concrete from pavement of a country area and after being extracted from the pavement it has been kept in the same conditions as AAC (Figure 3).

(a) (b)

Fig. 3. *The test material: (a) Autoclaved Aerated Concrete AAC; (b) Concrete*

The granular material with dimensions d < 40 mm (Figure 4) derived from aggregates of AAC and concrete and was considered part 2 and 3 for the batch leaching test according to EN 12457-2 respectively EN 12457-3. The part 2 consists in one stage batch leaching test, where the liquid-solid ratio is L/S = 10 L/kg, while the part 3 consists in two stage batch leaching tests, where the liquid-solid ratio is L/S = 2 L/kg in the first step and L/S = 8 L/kg in the second step.

THE ANNALS OF "DUNAREA DE JOS" UNIVERSITY OF GALATI
FASCICLE IX. METALLURGY AND MATERIALS SCIENCE
Nº. 2 - 2024, ISSN 2668-4748; e-ISSN 2668-4756
Article DOI: https://doi.org/10.35219/mms.2024.2.02

(a) (b)

Fig. 4. *The test granular material with d < 40 mm: (a) Autoclaved Aerated Concrete AAC; (b) Concrete*

The single stage batch leaching tests were performed with distilled water on two types of material with particle size < 4 mm and at an L/S-ratio of 10 L/kg. The distilled water and the construction material remained in contact for 24 hours (Figure 5). At the beginning of the contact period the solution of material and distilled water was stirred for 30 minutes and left in contact for 23 more hours after which it was stirred for another 30 minutes and thus it was completed the 24-hour contact period. After the leaching test, the solutions were filtrated through a 0.45 μm filter and the resulted eluates were analysed for a wide range of parameters.

The two steps batch leaching tests were performed with distilled water on two types of material with a particle size < 4 mm and at an L/S-ratio of 2 L/kg followed by an L/S-ratio of 8 L/kg which corresponded to an accumulated L/S-ratio of 10 L/kg. In the first leaching step (L/S 2 L/kg) the contact time was 6 hours and in the second leaching step (L/S 8 L/kg) the contact time was 18 hours corresponding to a total contact time between the solid material and the leaching of 24 hours.

Fig. 5. *The construction materials in contact for 24 hours at L/S = 10 L/kg*

In the first leaching step (L/S 2 L/kg) at the beginning of the 6-hour contact period (Figure 6) the solution was stirred for 30 minutes and left in contact for 5 more hours after which it was stirred for another 30 minutes and thus it was completed the 6-hour contact period. After the leaching test the solutions were filtrated through a 0.45 μm filter and thus resulted the eluates corresponding to the 6-hour contact time.

In the second leaching step (L/S 8 L/kg) at the beginning of the 18-hour contact period the solution was stirred for 30 minutes and left in contact for 17 more hours after which it was stirred for another 30 minutes and thus it was completed the 18-hour contact period. After the leaching test the solutions were filtrated through a 0.45 μm filter and thus resulted the eluates corresponding to the 18-hour contact time.

(a) (b)

Fig. 6. *The construction materials in contact at L/S = 2+8 L/kg: (a) for 6 hours; (b) for 18 hours*

THE ANNALS OF "DUNAREA DE JOS" UNIVERSITY OF GALATI
FASCICLE IX. METALLURGY AND MATERIALS SCIENCE
Nº. 2 - 2024, ISSN 2668-4748; e-ISSN 2668-4756
Article DOI: https://doi.org/10.35219/mms.2024.2.02

The eluates corresponding to the 6-hour contact time and 18-hour contact time were mixed and resulted the eluates for two-stage batch leaching test, which were analysed for a wide range of parameters.

The two sets of eluates were subjected to physic and chemical analysis, namely electrical conductivity, TDS (Total Dissolved Solid Materials), reaction (pH), temporary hardness, anions HCO_3^-, Cl^-, SO_4^{2-}, cations Ca^{2+}, Mg^{2+}. The analysis was carried out according to current standards, as shown in Table 3.

Table 3. *The standardized methods of analysis*

Indicator and measure unit	The analytical method
Conductivity µS/cm	potentiometric
TDS ppm	potentiometric
pH	potentiometric
Temporary hardness, ºd	titrimetric
HCO_3^-, mg/L	volumetric
Cl^-	titrimetric
SO_4^{2-}	volumetric
Ca^{2+}	titrimetric
Mg^{2+}	titrimetric

5. Conclusions

The test materials AAC and Concrete have a high Dissolved Solid Materials in eluates, but in case of AAC the two-stage batch leaching test lead to an increase with about 2000 mg/kg, while for Concrete lead to a decrease of about 900 mg/kg. Thus, in order to reduce the leaching of Dissolved Solid Materials from Concrete, the two-stage batch leaching test is appropriate.

The two-stage batch leaching test also led to the decrease of the eluates reaction (pH) for both materials, from strongly alkaline to moderately alkaline.

Although the concentration of sulphate ions is very high for both materials, the two-stage batch leaching test reduced them with about 1000 mg/kg for AAC and about 500 mg/kg for Concrete.

The HCO_3^- and Ca^{2+} ions had lower concentration in the two-stage batch leaching test. As for the Mg^{2+} ions and Cl^- ions, their concentration was lower in the two-stage batch leaching test for Concrete but was higher in the two-stage batch leaching test for AAC.

The two-stage batch leaching test was generally more beneficial for Concrete due to the decrease of all indicators value and less for AAC because the TDS indicator had a very important increase which may affect the ground of the landfill for inert waste. Thus, the leaching of solvable elements differs depending on the materials composition and their behavior in the leaching tests.

The solution for reducing the ground impact of the inert waste leachate is the three R – Reuse, Reduce, Recycle involving different methods such as reducing the CD waste by implementing installations for recovery of material fractions as close as possible to the generation source.

The future directions for research may consist in the analysis of the chemical characteristics of the test materials for different contact time and different number of leaching steps. According to these specific characteristics one can identify for which test materials the contact time and the number of leaching steps have major influence on the chemical elements' concentration in the leached amount. The topic of the study is very current and there is a great potential in terms of environmental impact evaluation. Some authors emphasize reducing the environmental impact of CD materials by reducing, recycling, incinerating with energy recovery and less by storing them on landfill.

References

[1]. ***, http://apmgl.anpm.ro/ro/dezvoltare-durabila.
[2]. ***, Policy Learning Platform, *Construction and demolition waste*, https://www.interregeurope.eu/policylearning/news/1770/construction-and-demolition-waste/.
[3]. ***. *Protocolul UE pentru gestionarea deșeurilor din construcții și demolări*, Septembrie 2016, http://ec.europa.eu/DocsRoom/documents/20509/attachments/1/translations/.
[4]. ***, *Service Contract on Management of Construction and Demolition Waste – SR1*, Final Report Task 2, February 2011, A project under the Framework contract ENV.G.4/FRA/2008/0112, European Commission (DG ENV), 2011.
[5]. ***, https://www.zf.ro/eveniment/reciclarea-deseurilor-din-constructii-si-demolari-in-romania-nu-exista-o-piata-totul-este-dezorganizat-unul-duce-la-groapa-altul-ascunde-16771877.
[6]. ***, *Towards a circular economy, Waste management in the EU*, STUDY Science and Technology Options Assessment, EPRS | European Parliamentary Research Service Scientific Foresight Unit (STOA) PE 581.913, http://www.europarl.europa.eu/RegData/etudes/STUD/2017/581913/EPRS_STU%282017%29581913_EN.pdf.
[7]. ***, Comunicat de presă, nr. 270, 15.10.2017, Institutul național de statistică din România, http://www.insse.ro/cms/ro/content/lucr%C4%83rile-de-construc%C8%9Bii-43.

THE ANNALS OF "DUNAREA DE JOS" UNIVERSITY OF GALATI
FASCICLE IX. METALLURGY AND MATERIALS SCIENCE
N°. 2 - 2024, ISSN 2668-4748; e-ISSN 2668-4756
Article DOI: https://doi.org/10.35219/mms.2024.2.03

3D PRINTING ERRORS DETECTION DURING THE PROCESS

Florin-Bogdan MARIN[1,2], Mihaela MARIN[1,2]
[1] "Dunarea de Jos" University of Galati, Romania
[2] Interdisciplinary Research Centre in the Field of Eco-Nano Technology and Advanced Materials CC-ITI, Faculty of Engineering, "Dunarea de Jos" University of Galati, 47 Domneasca Street, RO-800008, Galati, Romania
e-mail: flmarin@ugal.ro

ABSTRACT

Automated error detection in 3D printing is an important challenge that impacts not only the quality of the final parts but also operational efficiency, helping to minimize wasted time and material. Certain types of errors can even result in printer malfunctions. A widely used solution for monitoring the printing process involves employing a webcam to observe the process in real time, either alerting the operator or halting the print if an issue is detected. In this paper, a computer vision algorithm able to detect specific errors is proposed.

KEYWORDS: 3D printing, errors, detection, machine learning

1. Introduction

Unmanned error detection in 3D printing is a critical issue that affects not only the final quality of produced parts but also operational efficiency by reducing wasted time and material consumption. In many applications, printing errors can be caused by various factors such as: nozzle clogging [1-3], first-layer adhesion issues [4-5], irregular filament extrusion [6-7], positioning errors [8-9], or even mechanical failures of the printer [10].

Introducing a webcam into the printing process for real-time monitoring and error detection can significantly improve product quality and reduce waste.

3D printing errors can be classified into various categories: extrusion problems, nozzle clogging, delamination, layer shifting, print bed adhesion issues.

One of the most common solutions for monitoring printing is the use of a webcam that tracks the process in real time and alerts the operator or halts the print in case an error is detected [11, 12].

Video monitoring of the 3D printing process is an increasingly popular solution due to its simplicity and efficiency. Webcams are relatively inexpensive and can be easily integrated with 3D printers, providing a clear view of the process. These cameras can function in two main ways: active monitoring and image processing.

Active monitoring with automatic error detection allows the user to be informed by a system as a program using image processing algorithms or machine learning techniques to automatically analyse the images captured by the webcam and detect errors in real-time.

Image processing is a key technology for automatic error detection in 3D printing using a webcam [13-16]. By analysing the images captured during printing, an algorithm can compare the current progress with a reference model or a set of predefined conditions to identify deviations or anomalies.

There are two major approaches to image processing for error detection: featured-based analysis and machine learning algorithms.

In feature-based analysis, the approach focuses on detecting specific visual characteristics, such as layer shape, texture, thickness, or colour. If a feature does not match the expected one, the algorithm can detect an error.

A promising area for error detection in 3D printing is the use of machine learning algorithms [17-22]. These can be trained to recognize specific patterns of errors and to make predictions based on images captured by the webcam.

Several types of algorithms can be used for this purpose, such as convolutional neural networks (CNN), which are particularly effective in image analysis. Convolutional Neural Networks (CNN) are a class of deep learning algorithms that have proven to be extremely efficient in image recognition and visual analysis [23-28].

A CNN model can be trained to recognize different types of printing errors, such as nozzle

THE ANNALS OF "DUNAREA DE JOS" UNIVERSITY OF GALATI
FASCICLE IX. METALLURGY AND MATERIALS SCIENCE
Nº. 2 - 2024, ISSN 2668-4748; e-ISSN 2668-4756
Article DOI: https://doi.org/10.35219/mms.2024.2.03

clogging, layer shifting, or uneven filament extrusion, by being exposed to a dataset of appropriately labelled images. The process of training a CNN model begins with collecting a large set of images from 3D prints. These images are labelled to indicate the presence or absence of certain types of errors. The model is then trained to recognize patterns associated with these errors. After training, the model can analyse new images in real time and automatically detect errors. Once a convolutional neural network model has been trained and deployed, it can be integrated with the webcam to monitor the 3D printing process in real-time. The algorithm analyses each frame and detects anomalies that could signal the appearance of an error.

There are already several examples of projects and commercial solutions that use webcams and image processing technologies to detect errors in 3D printing. One of the most well-known examples is OctoPrint [29], an open-source platform that allows remote monitoring and control of 3D printers. OctoPrint can be integrated with webcams to provide real-time visual surveillance, and in some cases, it can be configured to stop printing if major errors such as layer shifting or extrusion problems are detected.

Another example is The Spaghetti Detective, [30] a plugin for OctoPrint that uses machine learning to detect printing errors. The term "Spaghetti" refers to a common type of error in 3D printing when the filament begins to tangle and form an uncontrolled mass resembling spaghetti. Spaghetti Detective uses a convolutional neural network [31] to analyse images captured by the webcam and detect such errors. If the algorithm detects an error, it can automatically halt the print and send an alert to the user.

In the future, as image processing technologies and machine learning algorithms become more advanced, we can expect an increase in the efficiency and accuracy of these systems. Additionally, it is likely that we will see their integration into more platforms and commercial solutions, making automatic error detection a standard feature of 3D printers.

Although there are some challenges related to image quality and the complexity of part geometry, these can be addressed by using higher-quality cameras and developing more advanced algorithms. In conclusion, implementing these webcam-based error detection systems has the potential to revolutionize the way 3D printing is performed, contributing to a more efficient, cost-effective, and reliable process.

This study aims to explore the ways in which a webcam can be used for error detection, analyse relevant image processing and machine learning technologies, and provide an overview of the most effective methods for implementing this technology in 3D printing. While this technology has brought many advantages, including design flexibility and the ability to produce complex parts, 3D printing often suffers from errors that can compromise the quality of the final product.

2. Experimental procedure

In Figure 1 it is shown the "spaghetti like" defect on the experimental setup. A webcam is placed on 3D printed in such a way to have the view towards the printer bad.

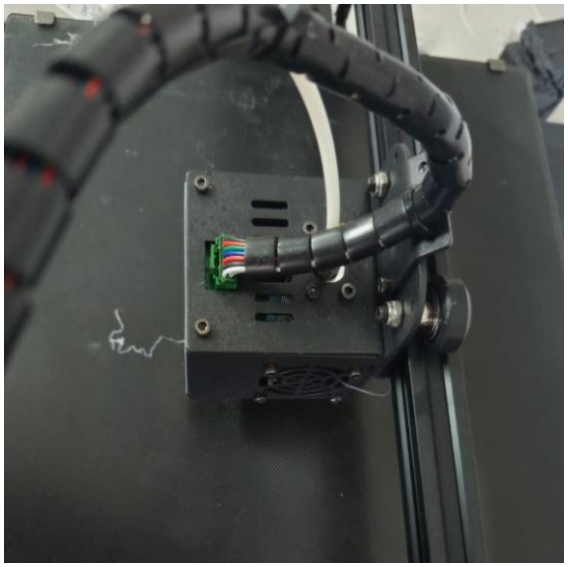

Fig. 1. *View from the webcam to be recognized*

Although error detection with webcams and image processing algorithms is a promising solution, it is not without challenges. One of the main limitations is image quality. A low-quality webcam may not be able to capture fine details, and under poor or variable lighting conditions, the accuracy of error detection may decrease significantly.

Another challenge is the complexity of printed models. Complex parts with detailed geometries and thin layers may be difficult for image processing algorithms to analyse. In some cases, small differences between the correct part and an error may be hard to detect, especially if the error occurs in less visible areas of the part (Figure 2).

An important aspect of using webcams for error detection is their integration with automated control systems for 3D printers. In this way, detecting an error can trigger automated actions such as stopping the print, adjusting printing parameters, or sending an alert to the user. The webcam constantly captures images, the image processing algorithm analyses them in real-time, and if an error is detected, the 3D printer receives a signal to stop the process. This type

THE ANNALS OF "DUNAREA DE JOS" UNIVERSITY OF GALATI
FASCICLE IX. METALLURGY AND MATERIALS SCIENCE
Nº. 2 - 2024, ISSN 2668-4748; e-ISSN 2668-4756
Article DOI: https://doi.org/10.35219/mms.2024.2.03

of automation not only improves the quality of the final products but also contributes to the optimization of time and resources. Using a webcam for error detection in 3D printing is an efficient and accessible solution for improving the quality and reliability of the additive manufacturing process. By utilizing image processing technologies and machine learning algorithms, this system can detect anomalies in real-time, preventing major defects and reducing material waste.

Fig. 2. *" Spagetti" errors pose variation*

In order to detect such defects, we want to create a custom architecture of DeepLabV3, by changing the number of Dilated Convolutions and the parameterization of the Atrous Spatial Pyramid Pooling (ASPP) module to suit our specific needs. Regarding the dilated convolutions we will change the dilation rates within some convolutional layers in the ResNet backbone to increase/decrease the receptive field. Also related to the ASPP (Atrous Spatial Pyramid Pooling) parameter, we will adjust the dilation rates and the number of convolutional modules in ASPP, to experiment with various levels of detail in capturing the spatial context.

Atrous Spatial Pyramid Pooling (ASPP) is a key component in convolutional neural network architectures used for semantic segmentation, as seen in DeepLab. ASPP is extremely useful for capturing spatial context at multiple scales from an image, allowing the model to understand both local details and global information. Using a customized ASPP brings flexibility depending on the specific application (in your case, detecting filaments in images).

3. Results and discussions

Semantic segmentation is the task of assigning a label to every pixel in an image to identify the objects present, and ASPP plays a crucial role in this process because capturing multi-scale context is of very high importance: Each dilated convolution in ASPP captures information from regions of different sizes in the image. A small dilation rate captures local details (such as edges and contours), while a larger dilation rate captures information from a broader area of the image, which is important for identifying the overall context. Minimizing loss of resolution is a paramount objective when dealing with ASPP as ASPP helps retain image details without losing resolution through excessive pooling, which is essential for capturing small or thin objects (such as the filaments in 3D printing processes). Objects in real-world images can vary in size and shape, and ASPP enhances the model's ability to detect these variations. We developed an architecture that allows a customized ASPP allows for adjusting the dilation rate and the number of convolutional blocks to better fit the characteristics of the data.

In filament detection, a precise segmentation of very thin and irregular objects is needed, and ASPP can be configured to give more attention to fine details by using smaller dilation rates in combination with larger rates to capture the overall context. By using smaller dilation rates for convolutional layers dedicated to local details can avoid losing critical details such as the edges of filaments or fine structures that may be essential for detecting them.

ASPP combines global and local information, which is essential for detecting filaments or small objects within the broader context of the image. This improves the model's accuracy in identifying objects that might be difficult to detect without considering the overall scene context. In the customized architecture we discussed, ASPP was configured with dilation rates of 6, 12, 18, and 24. These values are parameterized to allow for efficient multi-scale feature extraction. Small dilation (6) allows capturing local fine details, such as contours and small textures. In filament detection, this layer would be responsible for precisely identifying the filaments and other thin structures in the image. Medium dilation (12, 18) is ideal for capturing structures at an intermediate scale, such as filaments in the broader context of the printed object. These dilation rates can capture filaments that are spaced apart or span large areas of the image. Large dilation (24) helps capture information from very wide regions of the image and is useful for understanding the overall context. This layer is important for linking locally detected filaments to the general structure of the printed object.

THE ANNALS OF "DUNAREA DE JOS" UNIVERSITY OF GALATI
FASCICLE IX. METALLURGY AND MATERIALS SCIENCE
N°. 2 - 2024, ISSN 2668-4748; e-ISSN 2668-4756
Article DOI: https://doi.org/10.35219/mms.2024.2.03

For dilation rate of 6 we obtain 76 % detection rate, for 12 92 % detection rate, for 18 detection rate was 95 % while using 24 dilation rate we obtain only 88 %. The application was developed in Pytorch and it recognized the printing error as shown in Figure 3.

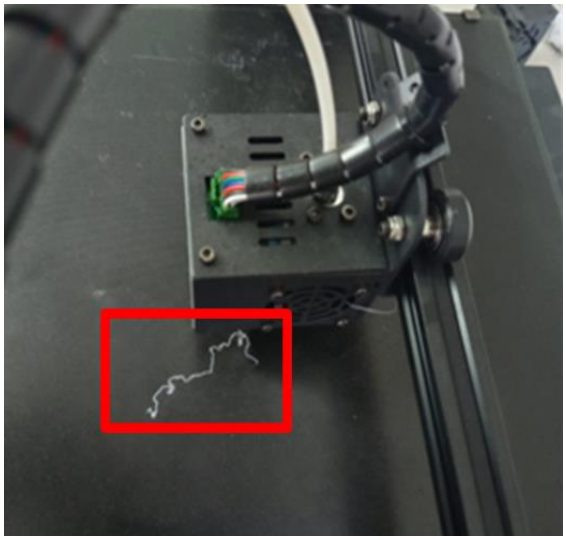

Fig. 3. *Detection of the error*

A well-configured ASPP with variable dilation rates can be crucial for improving performance in applications where detecting small and fine details is critical. Detecting filaments in images, especially in the context of 3D printing images, is a challenging task because filaments have irregular shapes and are often very thin. Smaller dilation rates in ASPP help in the precise segmentation of filaments that are very thin and could be lost in other segmentation approaches that do not use dilated convolutions.

4. Conclusions

Top customized ASPP is a powerful solution for improving the performance of semantic segmentation networks when detecting filaments or other thin and irregular formations.

By using variable dilations and capturing multi-scale context, ASPP allows neural networks to be efficient in capturing fine details and the overall context of the image.

In filament detection for processes such as 3D printing, a customized ASPP can provide a robust solution for accurately segmenting these thin objects and other complex structures, maintaining both local details and global context.

Adjusting the dilations and the number of ASPP blocks can be done to achieve the perfect balance between accuracy and performance, depending on the specific data and purpose of the application.

ASPP extends the receptive field without losing the fine details of the filaments. This allows the network to capture both the local filaments and the general distribution of filaments across the entire scene.

By creating convolutional layers at multiple scales, ASPP helps avoid over fitting on local details. Instead, capturing context at various scales allows the network to detect filaments without over fitting to noise present in the visual data.

Modifying the dilation rate in a customized ASPP can affect the model's ability to detect filaments, particularly depending on their geometry and distribution. ASPP improves the detection of these varied shapes without compromising segmentation precision.

References

[1]. Tlegenov Y., Soon G., Wen H., Lu F., *Nozzle condition monitoring in 3D printing*, Robotics and Computer-Integrated Manufacturing, 54, p. 45-55, 2018.
[2]. Shoukat A. K., *et al.*, *The impact of nozzle diameter and printing speed on geopolymer-based 3D-Printed concrete structures: Numerical modeling and experimental validation*, Results in Engineering, 21, 101864, p. 1-8, 2024.
[3]. Tlegenov Y., Lu W. F., Hong, G. S., *A dynamic model for current-based nozzle condition monitoring in fused deposition modelling*, Prog Addit Manuf, 4, p. 211-223, 2019.
[4]. Spoerk M., *et al.*, *Effect of the printing bed temperature on the adhesion of parts produced by fused filament fabrication*, Plastics, Rubber and Composites, 47:1, p.17-24, 2018.
[5]. Bakarzhiev V., *et al.*, *Research into 3d printing layer adhesion in ABS materials*, Environment. Technologies. Resources, Proceedings of the International Scientific and Practical Conference, 3, p. 41-45, 2023.
[6]. Guidetti X., *et al.*, *Force controlled printing for material extrusion additive manufacturing*, Additive Manufacturing, 89, 104297, p. 1-23, 2024.
[7]. Iftekar S. F., *et al.*, *Advancements and Limitations in 3D Printing Materials and Technologies: A Critical Review*, Polymers, 15, 2519, p. 1-23, 2023.
[8]. Li L., McGuan R., Isaac R., Kavehpour P., Candler R., *Improving precision of material extrusion 3D printing by in-situ monitoring & predicting 3D geometric deviation using conditional adversarial networks*, Additive Manufacturing, 38, 101695, p. 1-12, 2021.
[9]. Isiani A., *et al.*, *Fault Detection in 3D Printing: A Study on Sensor Positioning and Vibrational Patterns*, Sensors, 23(17), 7524, p. 1-29, 2023.
[10]. Scipioni S. I., Lambiase F., *Error introduced by direct 3D printing of compression samples of PLA made by FDM process*, Int J Adv Manuf Technol, 129, p. 4355-4368, 2023.
[11]. Holzmond O., Li X., *In situ real time defect detection of 3D printed parts*, Additive Manufacturing, 17, p. 135-142, 2017.
[12]. Ganitano G. S., Wallace S. G., Maruyama B., *A hybrid metaheuristic and computer vision approach to closed-loop calibration of fused deposition modeling 3D printers*, Prog Addit Manuf, 9, p. 767-777, 2024.
[13]. Wang Y., *et al.*, *Image Source Identification Using Convolutional Neural Networks in IoT Environment*, Wireless Communications and Mobile Computing, p. 1-12, 2021.
[14]. Heriyadi P., *et al.*, *Image Processing in 3D Printing Application: Study Case of Liver Organ*, International Seminar on Application for Technology of Information and Communication (iSemantic), Semarang, Indonesia, p. 372-376, 2022.

[15]. Straub J., *Initial work on the characterization of additive manufacturing (3D printing) using software image analysis*, Machines, 3(2), p. 55-71, 2015.
[16]. Okamoto T., Ura S., *Verifying the Accuracy of 3D-Printed Objects Using an Image Processing System*, J. Manuf. Mater. Process, 8, 94, p.1-21, 2024.
[17]. Ugandhar D., Shing C., *Automated Process Monitoring in 3D Printing Using Supervised Machine Learning*, Procedia Manufacturing, 26, p. 865-870, 2018.
[18]. Xijun Z., *et al.*, *Machine learning-driven 3D printing: A review*, Applied Materials Today, 39, p. 1-20, 2024.
[19]. Songyuan G., *et al.*, *Research status and prospect of machine learning in construction 3D printing*, Case Studies in Construction Materials, 18, p. 1-19, 2023.
[20]. Yakubu A., *et al.*, *Optimization of 4D/3D printing via machine learning: A systematic review*, Hybrid Advances, 6, p. 1-21, 2024.
[21]. Omairi A., Ismail Z. H., *Towards Machine Learning for Error Compensation in Additive Manufacturing*, Applied Sciences, 11(5), 2375, p. 1-27, 2021.
[22]. Goh G., *Applications of machine learning in 3D printing*, Materials Today: Proceedings, 70, p. 95-100, 2022.
[23]. Kumar K. K., *et al.*, *Fault detection on the 3-D printed objective surface by using the SVM algorithm*, Materials Today: Proceedings, p. 1-6, 2023.
[24]. Alafaghani A., *et al.*, *Experimental Optimization of Fused Deposition Modelling Processing Parameters: A Design-for-Manufacturing Approach*, Procedia Manufacturing, 10, p.791-803, 2017.
[25]. Valizadeh M., Wolff S. J., *Convolutional Neural Network applications in additive manufacturing: A review*, Advances in Industrial and Manufacturing Engineering, 4, 100072, p. 1-12, 2022.
[26]. Kaisar K., *et al.*, *Convolutional Neural Network-Based Defect Detection Technique in FDM Technology*, Procedia Computer Science, 231, p. 119-128, 2024.
[27]. Garland A., *et al.*, *Deep Convolutional Neural Networks as a Rapid Screening Tool for Complex Additively Manufactured Structures*, Additive Manufacturing, 35, 101217, p. 1-12, 2020.
[28]. Rachmawati S., *et al.*, *Fine-Tuned CNN with Data Augmentation for 3D Printer Fault Detection*, 13th International Conference on Information and Communication Technology Convergence (ICTC), p. 902-905, 2022.
[29]. ***, https://octoprint.org/download/.
[30]. ***, https://www.obico.io/the-spaghetti-detective.html.
[31]. ***, Petsiuk A. L., Pearce J. M., *Open source computer vision-based layer-wise 3D printing analysis*, Additive Manufacturing, 36, 101473, p. 1-17, 2020.

THE ANNALS OF "DUNAREA DE JOS" UNIVERSITY OF GALATI
FASCICLE IX. METALLURGY AND MATERIALS SCIENCE
No. 2 - 2024, ISSN 2668-4748; e-ISSN 2668-4756
Article DOI: https://doi.org/10.35219/mms.2024.2.04

A HEART RATE MONITORING AND NOTIFICATION SYSTEM USING ARDUINO PLATFORM

Alina-Maria MOCANU[1], Mihaela MARIN[1,2], Florin-Bogdan MARIN[1,2]
[1] "Dunarea de Jos" University of Galati, Romania
[2] Interdisciplinary Research Centre in the Field of Eco-Nano Technology and Advanced Materials CC-ITI, Faculty of Engineering, "Dunarea de Jos" University of Galati, 47 Domnească Street, RO-800008, Galaţi, Romania
e-mail: mihaela.marin@ugal.ro

ABSTRACT

Heart rate measurements are widely used for various purposes that require an accurate and reliable method to measure it. The most common method used is by ECG, which is widely available and non-invasive. Another non-invasive, photoplethysmography (PPG) technology can also be used to measure blood pressure and oxygen saturation.

KEYWORDS: heart rate, monitoring system, photoplethysmography, sensor, Arduino

1. Introduction

In order to enhance the patient care and people's quality life, biomedical engineering integrates the design and scientific abilities of engineering with the medical and biological sciences. The medical devices are intended to be used in illness detection, treatment, cure or prevention [1-9].

The number of people with different cardiovascular risk factors is expanding alarmingly [10]. In addition, the worldwide rate of cardiovascular malady is expanding as the world's population ages and as ways of life (and in this way chance components) in low and middle-income nations become more comparative to those of wealthier countries [11-13].

Identifying and monitoring individual risk factors, as well as aiding with lifestyle adjustments, are critical components of cardiovascular disease treatment.

Monitoring the patient's heart rate provides a positive contribution to the monitoring of cardiovascular disease. There are several procedures found in the literature for taking heart rate measurements on mobile phone applications [14-26]. These procedures can be through physical contact and non-contact. The photoplethysmography technology is used to measure blood pressure and oxygen saturation [27]. The heart rate sensor is used to identify changes in heart rate [28-31].

In this study, we aim to develop a wearable heart monitoring system, which could help heart patients to improve their quality of health and serve as a wake-up call for any serious heart problems. The system provides real-time heart rate monitoring, which, patients with cardiovascular disease could benefit of, by enabling early detection of heart irregularities.

2. Experimental procedure

Referring to the block diagram proposed in Figure 1, the heart monitoring system comprises a sensing unit and a receiving unit.

The detection unit consists of the photoplethysmograph sensor, the microprocessor and the Bluetooth transceiver module. The receiving unit is the mobile phone with Bluetooth connection. The Bluetooth module has 6 pins. State and En pins will not connect in this case, instead VCC, GND, TX and RX pins will be connected as illustrated in Figure 2. The pulse sensor records the pulse signal, and the microcontroller analyses the received signal.

The microcontroller performs the calculation, the decision and finally it will send the heart rate data to: the monitor serial of the Arduino IDE program, to the OLED screen and to the Bluetooth module, following mobile phone connected to this module to receive the transmitted data (Figure 3).

THE ANNALS OF "DUNAREA DE JOS" UNIVERSITY OF GALATI
FASCICLE IX. METALLURGY AND MATERIALS SCIENCE
N°. 2 - 2024, ISSN 2668-4748; e-ISSN 2668-4756
Article DOI: https://doi.org/10.35219/mms.2024.2.04

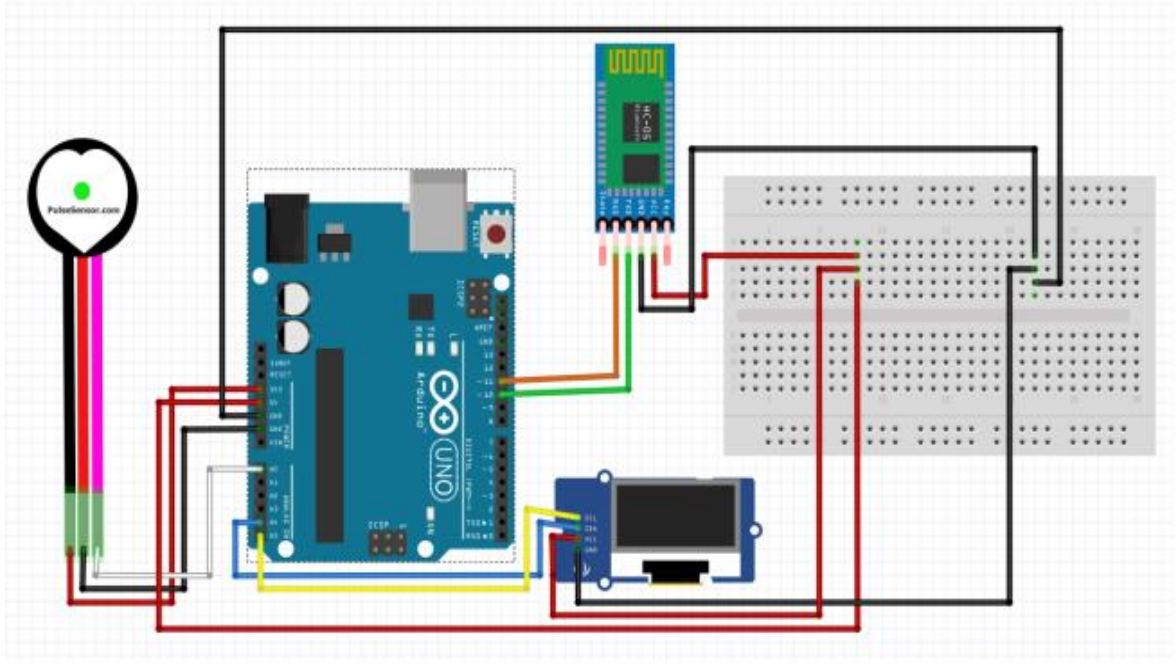

Fig. 1. *Block diagram of the proposed system architecture*

The microcontroller consists of a central processing unit (CPU), memory and various peripheral devices. The typical function of the microcontroller is to read the received data, perform calculations and control the environment based on the calculated data.

The standard pulse sensor SEN-11574 has three pins: Signal (S), VCC(+) and GND(-). According to the properties of this sensor, if the heart beats, then there is a change in voltage and vice versa. By connecting the test pin with the logic state, the change in the heart rate occurs. Therefore, if the test pin is set too high, it means that the finger is placed on the sensor, it detects the change in pulse and then the sensor gives a specific beat of the heart in the form of voltage (5V). Also, if the logic state is set low, it will not give any output voltage. This idea is further extended by replacing the logical state with a variable resistor. By setting the value of the resistor, the voltage is controlled, which means the sensor will give different readings in signal form (Figure 3). In Figure 4, the system architecture of heart rate monitoring device developed in this research is represented.

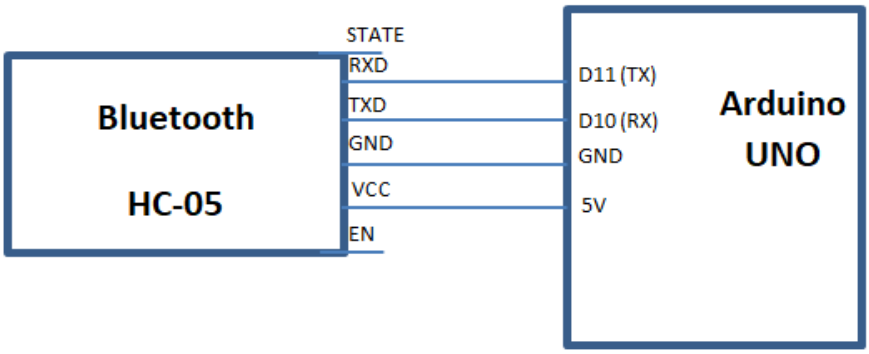

Fig. 2. *The pins connection between Bluetooth module HC-05 and microcontroller Arduino UNO*

THE ANNALS OF "DUNAREA DE JOS" UNIVERSITY OF GALATI
FASCICLE IX. METALLURGY AND MATERIALS SCIENCE
N°. 2 - 2024, ISSN 2668-4748; e-ISSN 2668-4756
Article DOI: https://doi.org/10.35219/mms.2024.2.04

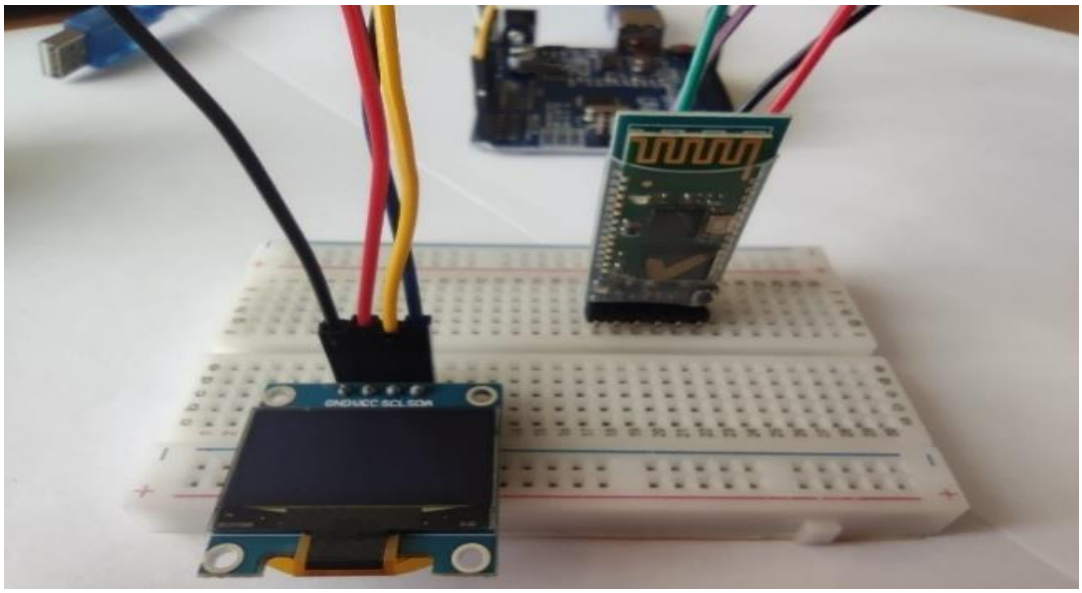

Fig. 3. *Connecting the OLED screen and the Bluetooth module to the breadboard*

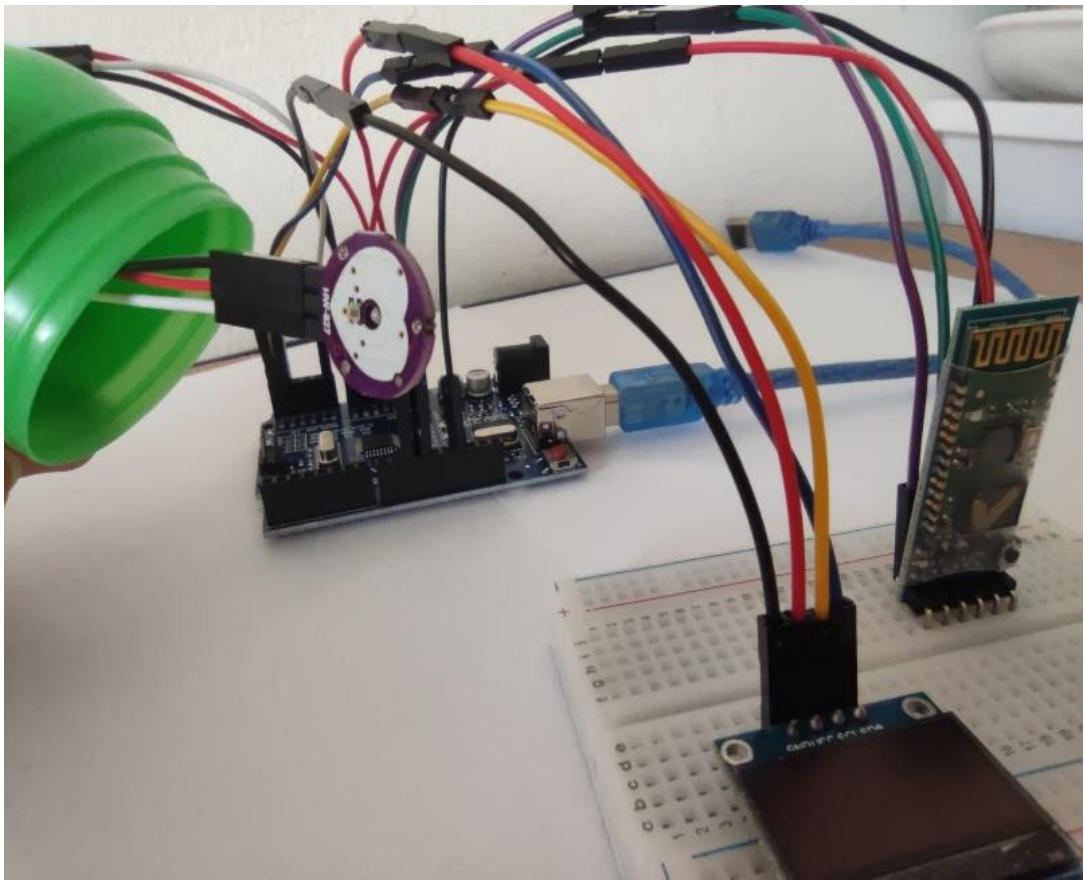

Fig. 4. *The system architecture of heart rate monitoring device*

3. Results and discussions

Once the components are connected, the USB cable must be mounted between the Arduino board and the laptop. The following will be selected from the Arduino menu: the corresponding port and the board, then to test the created code, press the Verify button, which compiles the code, to find the errors

THE ANNALS OF "DUNAREA DE JOS" UNIVERSITY OF GALATI
FASCICLE IX. METALLURGY AND MATERIALS SCIENCE
N°. 2 - 2024, ISSN 2668-4748; e-ISSN 2668-4756
Article DOI: https://doi.org/10.35219/mms.2024.2.04

and be able to solve them. The code steps are: introducing libraries, defining variables, and the two essential functions, void setup and void loop. In Figure 5, the initialization stage of serial monitor, Bluetooth module and OLED screen is presented. After the initialization stage, the actual functions follow, where information is calculated and conditions can be set. The next step in the void loop function is to make the display part, for the 3 types of monitors. This part is done with the loop function, the principle of a loop, precisely to continuously calculate the values of the pulse and to repeat the commands.

The monitoring system display and the results on the OLED screen and phone app Ardutooth are presented in Figure 6.

The results verification methodology is necessary to ensure the accuracy, sensitivity, specificity and precision of the heart rate monitor. The device output verification procedure includes comparing the device output values to the output values from an existing heart monitoring device.

In Figure 7 it can be seen how the value recorded at that time by the pulse sensor integrated in the developed system is in accordance with the value recorded by the pulse oximeter.

```
20  void setup()
21  {
22    display.begin(SSD1306_SWITCHCAPVCC, OLED_ADDR);
23    Serial.begin(9600);
24    B.begin(9600);
25
```

Fig. 5. *The initialization stage in the Arduino platform*

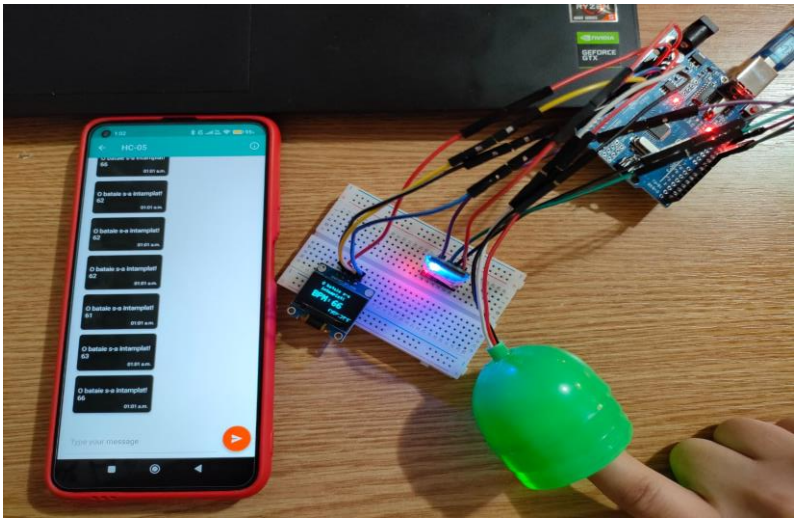

Fig. 6. *Monitoring the system display and the results on the OLED screen and phone app*

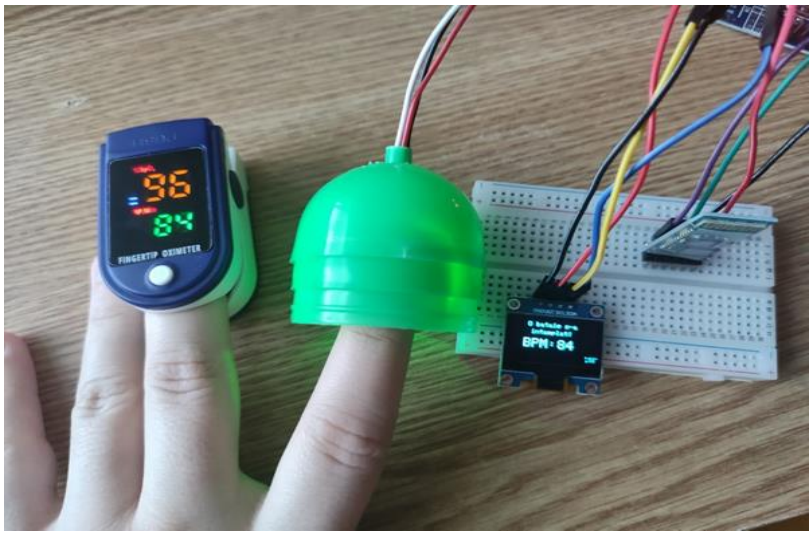

Fig. 7. *The results validation for the heart rate system proposed using a pulse oximeter*

THE ANNALS OF "DUNAREA DE JOS" UNIVERSITY OF GALATI
FASCICLE IX. METALLURGY AND MATERIALS SCIENCE
N°. 2 - 2024, ISSN 2668-4748; e-ISSN 2668-4756
Article DOI: https://doi.org/10.35219/mms.2024.2.04

4. Conclusions

This study integrates engineering design and problem solving with biomedical sciences to improve wearable heart monitoring systems, which could help heart patients improve their quality of health and serve as a wake-up call for any serious heart problems. The pulse monitoring system uses the principle of photoplethysmography (PPG) to detect heart rate values. By compiling proper coding for heart rate detection on the Arduino board, the results showed that heart rate could be detected from variations in blood flow in the finger.

The pulse sensor (SEN-11574) effectively detects heartbeats, and the validation process against a pulse oximeter confirms the accuracy of the developed system.

Using Bluetooth technology, the heart rate data is transmitted in real-time to a connected mobile phone, allowing for continuous monitoring.

By offering real-time alerts, the system helps improve response times to irregular heartbeats, potentially preventing serious health consequences for patients with cardiovascular conditions.

Moreover, such systems can also be implemented in hospitals or clinics for continuous patient monitoring by using wireless communication system.

References

[1]. Kasoju N., *et al.*, *Digital health: trends, opportunities and challenges in medical devices, pharma and bio-technology*, CSIT, 11, p. 11-30, 2023.
[2]. Yan Y., *et al.*, *The Present Clinical Treatment and Future Emerging Interdisciplinary for Heart Failure: Where we are and What we can do*, Intensive Care Res, 3, p. 3-11, 2023.
[3]. Russo A., *et al.*, *New advances in management and treatment of cardiac implantable electronic devices infections*, Infection, 52, p. 323-336, 2024.
[4]. Sharma A., *et al.*, *Health care policy and regulatory implications on medical device innovations: a cardiac rhythm medical device industry perspective*, J Interv Card Electrophysiol, 36, p. 107-117, 2013.
[5]. Lang M., *Heart Rate Monitoring Apps: Information for Engineers and Researchers About the New European Medical Devices Regulation*, JMIR Biomed Eng, 2(1), p. 1-5, 2017.
[6]. Arandia N., *Embedded Sensor Systems in Medical Devices: Requisites and Challenges Ahead*, Sensors, 22, (24), 9917, p. 1-28, 2022.
[7]. Khera R., *et al.*, *Transforming Cardiovascular Care with Artificial Intelligence: From Discovery to Practice: JACC State-of-the-Art Review*, JACC., 84, (1), p. 97-114, 2024.
[8]. McBeath K. C. C., *et al.*, *Digital Technologies to Support Better Outcome and Experience of Care in Patients with Heart Failure*, Curr Heart Fail Rep, 19, p. 75-108, 2022.
[9]. Tettey F., *et al.*, *A Review of Biomedical Devices: Classification, Regulatory Guidelines, Human Factors, Software as a Medical Device, and Cybersecurity*, Biomedical Materials & Devices, p. 1-27, 2023.
[10]. Mensah G. A., *et al.*, *Global Burden of Cardiovascular Diseases and Risks Collaborators. Global Burden of Cardiovascular Diseases and Risks, 1990-2022*, J Am Coll Cardiol., 82, (25), p. 2350-2473, 2023.
[11]. Gaziano T. A, *et al.*, *Growing epidemic of coronary heart disease in low- and middle-income countries*, Curr Probl Cardiol, 35, (2), p. 72-115, 2010.
[12]. Amini M., *et al.*, *Trend analysis of cardiovascular disease mortality, incidence, and mortality-to-incidence ratio: results from global burden of disease study 2017*, BMC Public Health, 21, 401, p. 1-12, 2021.
[13]. Wurie H. R., Cappuccio F. P., *Cardiovascular disease in low- and middle-income countries: an urgent priority*, Ethn Health, 17, (6), p.543-550, 2012.
[14]. De Ridder B., *et al.*, *Smartphone Apps Using Photoplethysmography for Heart Rate Monitoring: Meta-Analysis*, JMIR Cardio, 2, (1), p. 1-17, 2018.
[15]. Pipitprapat W., *et al.*, *The validation of smartphone applications for heart rate measurement*, Annals of Medicine, 50, (8), p. 721-727, 2018.
[16]. Bae S., *et al.*, *Prospective validation of smartphone-based heart rate and respiratory rate measurement algorithms*, Commun Med (Lond), 12, 2, 40, p. 1-11, 2022.
[17]. Ventola C. L., *Mobile devices and apps for health care professionals: Uses and benefits*, Pharm Ther., 39, (5), p. 356-364, 2014.
[18]. Dute D. J., *et al.*, *Using Mobile apps to promote a healthy lifestyle among adolescents and students: A review of the theoretical basis and lessons learned*, JMIR mHealth uHealth, 4, (2), p. 1-15, 2016.
[19]. Coppetti T., *et al.*, *Accuracy of smartphone apps for heart rate measurement*, European Journal of Preventive Cardiology, 24, (12), p. 1287-1293, 2017.
[20]. Garcia J., *et al.*, *Reviewing Mobile Apps to Control Heart Rate in Literature and Virtual Stores*, Journal of Medical Systems, 43, p. 1-9, 2019.
[21]. Gregoski M. J., *et al.*, *Development and validation of a smartphone heart rate acquisition application for health promotion and wellness telehealth applications*, Int J Telemed Appl., p. 1-7, 2012.
[22]. Kwon S., *et al.*, *Validation of heart rate extraction using video imaging on a built-in camera system of a smartphone*, Annu Int Conf Eng med. Biol. Soc., p. 2174-2177, 2012.
[23]. Sukaphat S., *et al.*, *Heart Rate Measurement on Android Platform*, 13th Int Conf Electr Eng Comput Telecommun Inf Technol., p. 1-5, 2016.
[24]. Bolkhovsky J. B., *et al.*, *Statistical analysis of heart rate and heart rate variability monitoring through the use of smart phone cameras*, Annu Int Conf Eng Med Biol Soc (EMBC), p. 1610-1613, 2012.
[25]. Lamonaca F., *et al.*, *Reliable pulse rate evaluation by smartphone*, IEEE Symp Med Meas Appl Proc MeMeA., p. 234-237, 2012.
[26]. Papon M. T. I., *et al.*, *Noninvasive heart rate measuring smartphone applications using onboard cameras: A short survey*, Proc Int Conf Netw Syst Secur NsysS, p. 1-6, 2015.
[27]. Allen J., *Photoplethysmography and its application in clinical physiological measurement*, Physiol. Meas., 28 R1, p. 1-40, 2007.
[28]. Galli A., *et al.*, *An Overview of the Sensors for Heart Rate Monitoring Used in Extramural Applications*, Sensors (Basel), 26, 22, (11), 2022.
[29]. Alugubelli N., *et al.*, *Wearable Devices for Remote Monitoring of Heart Rate and Heart Rate Variability - What We Know and What Is Coming*, Sensors, 22, 8903, p. 1-22, 2022.
[30]. Takahashi Y., *et al.*, *Accuracy of Heart Rate and Respiratory Rate Measurements Using Two Types of Wearable Devices*, Prog Rehabil Med, 7, p. 1-8, 2022.
[31]. De Pinho Ferreira N., *et al.*, *A Review of Methods for Non-Invasive Heart Rate Measurement on Wrist*, IRBM, 42, 1, p. 4-18, 2021.

THE ANNALS OF "DUNAREA DE JOS" UNIVERSITY OF GALATI
FASCICLE IX. METALLURGY AND MATERIALS SCIENCE
Nº. 2 - 2024, ISSN 2668-4748; e-ISSN 2668-4756
Article DOI: https://doi.org/10.35219/mms.2024.2.05

THE INFLUENCE OF CHEMICAL COMPOSITION ON COBALT-BASED ALLOYS

Mirabela Georgiana MINCIUNA[1,2], Petrică VIZUREANU[1,2]
[1] "Gheorghe Asachi" Technical University of Iasi, Faculty of Materials Science and Engineering, Blvd. Mangeron, No. 51, 700050, Iasi, Romania
[2] Centre of Excellence Geopolymer and Green Technology (CEGeoGTech), Universiti Malaysia Perlis (UniMAP), 01000 Perlis, Malaysia
e-mail: mirabela.minciuna@yahoo.ro

ABSTRACT

Cobalt-based alloys contain up to 50% cobalt, which means that they provide the material with increased abrasion resistance at high temperatures. Cobalt is similar to nickel because it is a hard material that is very resistant to wear and corrosion, especially at high temperatures. It is generally used as an element in alloys, due to its resistance to corrosion, but also due to its magnetic properties. In all cases, the introduction of an implant into an organism is likely to induce chemical, mechanical, electrical, thermal, magnetic and atomic interactions.

KEYWORDS: dilatometric analysis, cobalt, spectrometry, silicon

1. Optical emission spectrometry

The chemical composition was determined by optical emission spectrometry for two cobalt-based alloys (CoCrMo and CoCrSi). Preparation of the samples for optical emission spectrometry was performed by sanding with coarse-grained abrasive paper. The electronic discharge is done with the removal of a large amount of energy, which causes the formation of plasma and the emission of light. The light spectrum is divided by means of an optical diffraction network, and the results are processed with the help of specialized software. Since the discharge is at the surface of the sample and does not penetrate the sample, contamination of the sample surface is also measured.

The determined mass concentrations of the elements in the cobalt-based alloys are specified in Table 1.

Table 1. *The chemical composition of the alloys expressed in mass percentages*

Alloying element	CoCrMo	CoCrSi
	(mass %)	
Co	62.10	56.70
Cr	26.79	26.23
Mo	6.00	5.29
Ni	2.90	2.84
Si	0.78	7.40
Mn	0.42	0.39
Fe	0.33	0.58
Other	0.68	0.57

THE ANNALS OF "DUNAREA DE JOS" UNIVERSITY OF GALATI
FASCICLE IX. METALLURGY AND MATERIALS SCIENCE
Nº. 2 - 2024, ISSN 2668-4748; e-ISSN 2668-4756
Article DOI: https://doi.org/10.35219/mms.2024.2.05

Research on the chemical composition has highlighted the fact that the main elements identified in cobalt-based alloys are the following: Co, Cr, Si. For the analysed alloys, the determined chemical composition certifies that the percentage of silicon has increased, according to the values presented in Table 2.

Table 2. *Values determined by optical emission spectrometry*

Alloys	CoCrMo	CoCrSi
Silicon, [%]	0.78	7.40

By increasing the percent of silicon, the alloying elements showed lower values, a significant change being in the main element, cobalt. If it was initially found in a percent of 62.10% in the CoCrMo alloy, it came to be found in a 56.4% in the CoCrSi alloy. After the sampling, preparation and chemical attack of the samples, from cobalt-based alloys, we made chemical composition determinations using the EDX detector, type Quantax QW2, attached to the Vega Tescan LSH II electron microscope. The determined compositions are in points on the surface of the sample, after they have been previously prepared by grinding (on all types of abrasive paper) and polishing. The Table 3 presents the elemental composition in mass percentages evaluated from the EDX spectra of the samples, which allow highlighting the presence of cobalt on the surface, but also of the alloying element, silicon, plus a series of alloy component elements. The average elemental composition for cobalt, chromium, molybdenum and silicon was evaluated from EDX analysis of CoCrMo and CoCrSi alloys. This highlights the existence of silicon in varying percentages in cobalt-based alloys. The qualitative and quantitative chemical analysis (EDX) carried out on the alloys, confirms the increase in the percentage of silicon from 1.92 % as the CoCrMo alloy initially had, to a value of 6.40 for the CoCrSi alloy.

Table 3. *Chemical composition of the alloys, determined by EDX*

CoCrMo			CoCrSi		
Element	**Chemical composition (mass %)**	**Error (%)**	**Element**	**Chemical composition (mass %)**	**Error (%)**
Cobalt	60.85	1.72	**Cobalt**	28.05	0.80
Chromium	27.06	0.86	**Chromium**	60.47	1.62
Molybdenum	6.59	0.39	**Silicon**	6.40	0.33
Silicon	1.92	0.20	**Molybdenum**	5.45	0.26

Due to the short analysis time and the accuracy of the method, optical emission spectrometry is considered the most effective analysis method in controlling the elaboration of cobalt-based alloys, being able to further establish the mechanical processing required by the field of use of the materials (medicine). With the increase in the percentage of silicon, certified by the two analyses (optical emission spectrometry and qualitative and quantitative analysis (EDX)), the properties of cobalt-based alloys can be improved, having the obligation to remove the general disadvantages encountered in the case of classic alloys such as: low resistance to corrosion, modulus of elasticity higher than that of bone, but also low biocompatibility with human tissues.

2. Dilatometric analysis

The dilatometric analysis is based on the appearance of deviations on the expansion-temperature curves, more precisely from the normal spectrum of these curves, from the transformation temperatures, deviations caused by the dimensional changes of the parts [2]. Differential dilatometric curves are used to determine the transformation points, being the most frequently used method, while absolute dilatometric curves are used to determine the real expansion coefficient and transformation points. The purpose of the experiments is to record the length variation (Δl) that a sample tolerates, when it is subjected to heating at a certain temperature [4]. Under the specified conditions, we decided that the dilatometric analyses should not be performed only for the field of use of cobalt-based alloys, the experimental tests covering all the temperatures reached during the technological phases necessary for the manufacture of a skeletal partial prosthesis. There is a close relationship between the coefficient of thermal expansion and the melting point of the alloys in the CoCrMo system. The alloys subjected to experimental research have high melting temperatures, falling within the range of 1330-1400 °C [6]. In this analysis, the melting temperature is high and the coefficient of expansion is low, the reason being due to strong interatomic bonds. In the situation where the tooth and the restorative material

THE ANNALS OF "DUNAREA DE JOS" UNIVERSITY OF GALATI
FASCICLE IX. METALLURGY AND MATERIALS SCIENCE
N°. 2 - 2024, ISSN 2668-4748; e-ISSN 2668-4756
Article DOI: https://doi.org/10.35219/mms.2024.2.05

made of the CoCrMo alloy system have different expansion coefficients, then the materials will expand and contract differently, which will result in unwanted leaks and sliding of the restorative material against the tooth. The melting range of the alloys in the CoCrMo system must be at least 150-200 °C higher than the firing temperature of the ceramic masses. Ceramic masses that burn on alloys belong to the category of those with a low sintering range (850-1100 °C), to ensure easy processing, the melting range of the alloys is indicated to be below 1400 °C, a category in which the alloys ours fit perfectly. The dilatometric analysis was performed with the help of a Linseis L75H/1400 type differential dilatometer. Cobalt alloys subjected to dilatometric analysis have plane-parallel ends, and the section is square, with a side of 5 mm and a sample length of 30 mm, dimensions that fall within the standards of the dilatometer. The alloys from the CoCrMo system were placed on the sample holder where they were linearly heated. The modified length was transmitted via a quartz rod to a displacement transducer. The temperature of the sample was recorded by means of a thermocouple [6]. The heating of the standard samples was carried out in a tubular furnace, with electric resistance, up to the maximum temperature of 1200 °C, the heating speed of the sample was 10 °C/min, the cooling speed of the furnace being influenced by the cooling system with water that has a water flow rate of 5 m^3/h.

Fig. 1. *Linseis L75H/1400 dilatometer*

The use of small samples usually ensures a better precision of temperature regulation and the repeatability of the results, while large samples favour a better precision regarding the determination of elongation [8]. Figure 1 shows the thermal expansion of the specimen made of an alloy from the CoCrMo system, specific to partially skeletonized prostheses. The maximum thermal expansion reached by the sample at a temperature of 1200 °C is 377 µm.

The Table 4 shows the elongation variation depending on the heating temperature for the CoCrMo alloy.

The behavior of the CoCrSi alloy is shown in Figure 3. It shows a linear and uniform expansion. The CoCrSi alloy shows an elongation of 290 µm at a temperature of 1200 °C.

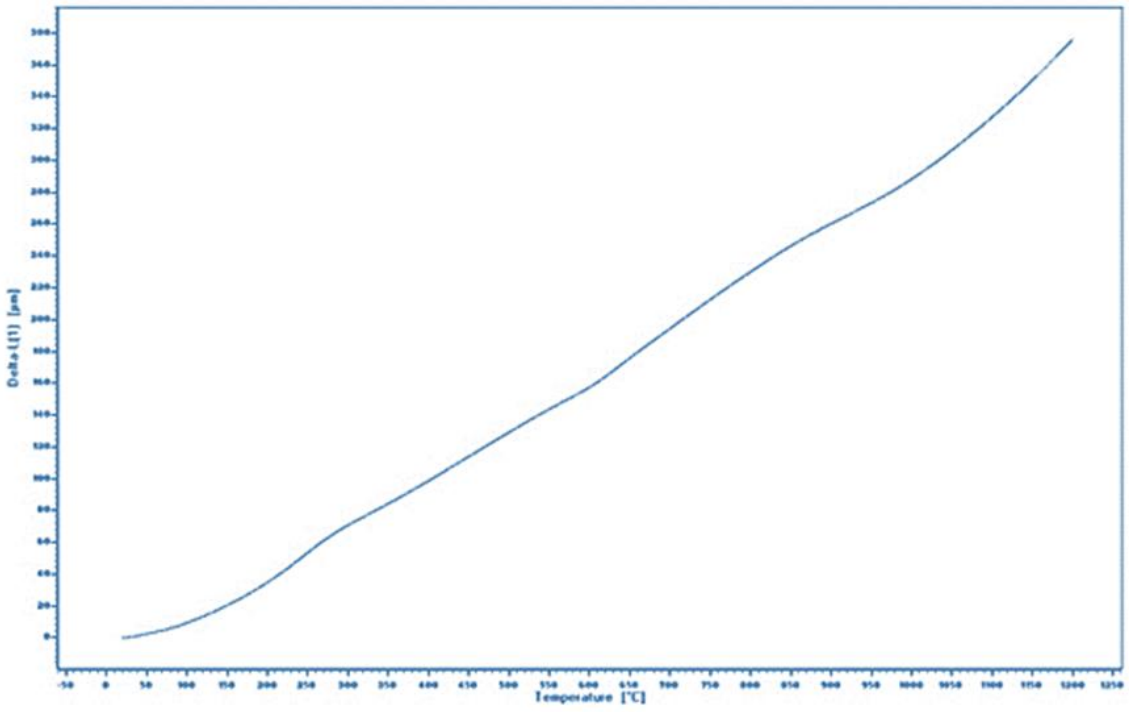

Fig. 2. *Variation of elongation with temperature, for the CoCrMo alloy*

THE ANNALS OF "DUNAREA DE JOS" UNIVERSITY OF GALATI
FASCICLE IX. METALLURGY AND MATERIALS SCIENCE
No. 2 - 2024, ISSN 2668-4748; e-ISSN 2668-4756
Article DOI: https://doi.org/10.35219/mms.2024.2.05

Table 4. *Elongation values as a function of temperature for the CoCrMo alloy*

Temperature [ºC]	20	190	290	400	550	650	750	850	1000	1100	1200
Elongation [µm]	0	31	68	97	140	180	215	235	280	330	380

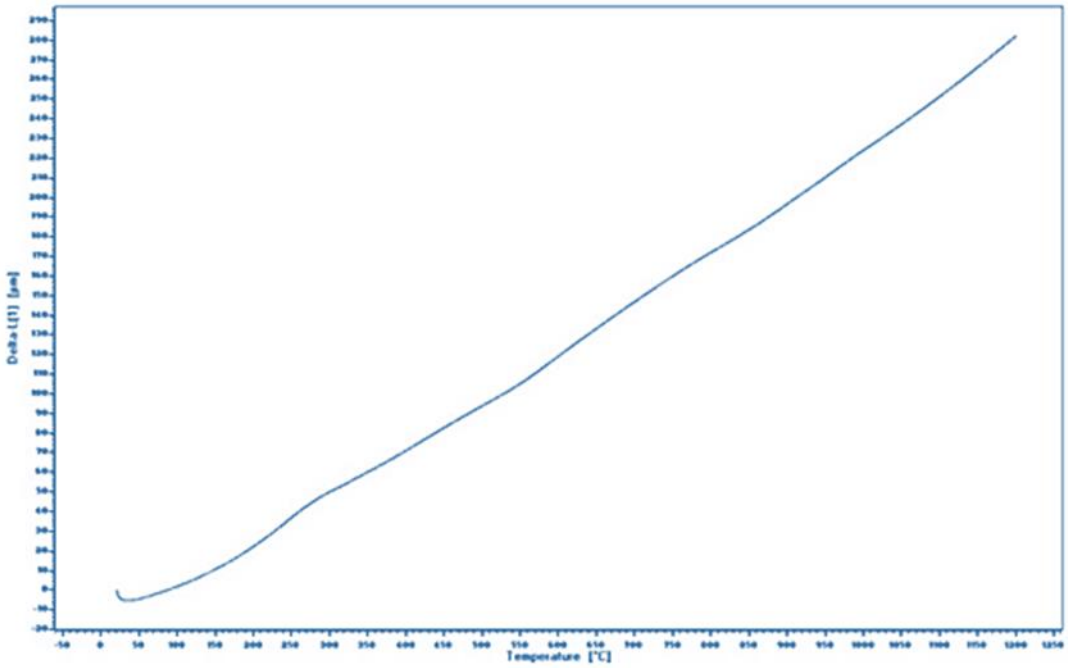

Fig. 3. *Variation of elongation with temperature, for the CoCrSi alloy*

Table 5. *Elongation values as a function of temperature for the CoCrSi alloy*

Temperature [ºC]	20	150	280	380	450	570	670	780	950	1050	1200
Elongation [µm]	0	12	46	66	83	111	141	168	207	242	290

The most pronounced thermal expansion, with a value of 380 µm, is presented by the sample made from the CoCrMo alloy system, instead the CoCrSi alloys obtained elongation values below 290 µm, which confirms that increasing the percentage of silicon improved the coefficient of thermal expansion. In the case of alloys from the CoCrMo system, it is important to know the value of the coefficient of thermal expansion α for the following reasons:

- the value of the coefficient should be reduced in order to keep the tolerances of the implant constant;
- the value of the coefficient of the metal implant to be correlated with that of the biological materials with which it comes into contact.

3. Conclusions

Chemical composition research has shown that the main elements identified in cobalt-based alloys are Co, Cr, Mo and the element Si. By increasing the percentage of silicon, the alloying elements showed lower values, a significant change being in the main element, cobalt. If it was initially found in a percentage of 62.1 % in the CoCrMo alloy, it came to be found in a percentage of 56.4% in the CoCrSi alloy. With the help of dilatometric analysis, we obtained the 'thermal elasticity' of cobalt-based alloys. The fact that no inflection points appear on the dilatograms confirms that there are no phase transformations in the solid state, thus we are certain of a stable behavior in the average ambient temperature range – 1200 °C, of the two analysed alloys. The analysed CoCrMo and CoCrSi alloys obtained elongation values below 290 µm, which confirms that increasing the percentage of silicon improved the coefficient of thermal expansion.

References

[1]. Henriques B., Silva F., Soares D., J. Mech. Behav. Biomed. Mater., 4, (8), p. 1718-1726, 2011.
[2]. Nowacki J., Pieczonka T., *Dilatometric analysis of sintering of iron–boron–cobalt P/M metal matrix composites*, Journal of

Materials Processing Technology, vol. 157-158, p. 749-754, Achievements in Mechanical and Materials Engineering Conference, 20 December 2004.
[3]. Li W., Lee L. J., *Low temperature cure of unsaturated polyester resins with thermoplastic additives: I. Dilatometry and morphology study*, Polymer, vol. 41, Issue 2, p. 685-696, January 2000.
[4]. Bobby R. Lanier, *et al.*, *Making chromium-cobalt removable partial dentures: A modified technique*, The Journal of Prosthetic Dentistry, vol. 25, Issue 2, p. 197-205, 1971.
[5]. Bernhard Wunderlich, *Chapter 6 - thermomechanical analysis and dilatometry*, *Thermal Analysis*, p. 311-369, 1990.
[6]. Moon J. H., Won D. M., *Analysis of sintering kinetics at different heating rates by dilatometry*, Metal Powder Report, vol. 55, Issue 2, p. 39, February 2000.
[7]. Sam Katz, *Dilatometry*, *Methods in Enzymology*, vol. 26, p. 395-406, 1972.
[8]. ***, www.academia.edu/4713685/ALIAJE_DENTARE.
[9]. Baba N., *et al.*, *Mechanical strength of laser-welded cobalt-chromium alloy*, J Biomed Mater Res B, 69B, p. 121-124, 2004.
[10]. Bagby M., *et al.*, *Metal Ceramic compatibility*, J Prosthet Dent. 63, p. 21-25, 1990.
[11]. Behazin M., *et al.*, *Combined Effects of pH and γ-Irradiation on the Corrosion of Co-Cr Alloy Stellite-6*, Electrochimica Acta, vol. 134, p. 399-410, 2014.
[12]. Baciu E. R., Forna N. C., *Influenţa tehnicilor de finisare asupra rugozităţii suprafeţelor componentelor metalice ale restaurărilor protetice*, Revista Medico-Chirurgicală a Societăţii de Medici şi Naturalişti din Iaşi, vol. 114, no. 4, ISSN: 0048-7848, p. 1198-2003, 2010.
[13]. Bollen C. M., Lambrechts P., Quirynen M., *Comparison of surface roughness of oral hard materials to the threshold surface roughness for bacterial plaque retention: a review of the literature*, Dent Mater, 13, p. 258-69, 1997.
[14]. Black J., Hastings G. W., *Handbook of Biomaterial Properties*, Chapman & Hall, 1998.
[15]. Bezzon O. L., *et al.*, *Effect of casting technique on surface roughness and consequent mass loss after polishing of (Ni-Cr) and (Co-Cr) base metal alloys: a comparative study with titanium*, J Prosthet Dent, 92, p. 274-279, 2004.
[16]. Bojin D., *et al.*, *Microscopie electronică de baleiaj şi aplicaţii*, Ed. Agir, Bucureşti, 2005.
[17]. Barbosa F. O., Araújo M. C., *Fractographic Analysis of K3 Nickel-Titanium Rotary Instruments Submitted to Different Modes of Mechanical Loading*, Journal of Endodontics, vol. 34, Issue 8, p. 994-998, 2008.
[18]. Black J., Hastings G. W., *Handbook of Biomaterial Properties*, Chapman & Hall, 1998.
[19]. Baynes J., Domniczak M. K., *Medical Biochemistry*, St. Louis: Mosby, ISBN 0723430128, 1999.

THE ANNALS OF "DUNAREA DE JOS" UNIVERSITY OF GALATI
FASCICLE IX. METALLURGY AND MATERIALS SCIENCE
Nº. 2 - 2024, ISSN 2668-4748; e-ISSN 2668-4756
Article DOI: https://doi.org/10.35219/mms.2024.2.06

STUDY REGARDING THE SIMULATION OF THE FLOW OF A FLUID THROUGH PIPES INTENDED FOR THE DOMESTIC WATER NETWORK, AND THE CAUSES OF THEIR DEGRADATION

Beatrice Daniela TUDOR, Dumitra STERIAN
"Dunarea de Jos" University of Galati, Romania
e-mail: beatrice.tudor@ugal.ro

ABSTRACT

A public water supply and sanitation system refers to the infrastructure and services needed to provide drinking water, and to collect and treat wastewater, in a community or geographic area. It has the role of ensuring access to safe drinking water and correctly managing liquid waste generated by the population and industry.

The paper makes a simulation, with the help of the SolidWorks program, of the flow of liquids through the pipes, and analyses the causes of the degradation of the pipes, intended for the domestic water network.

KEYWORDS: simulation, flow, degradation, program

1. General information on the water supply system

A water supply system is an important component of the hydrotechnical system, and has the role of providing drinking water, or water for other purposes, in a certain area or populated centre. It is made up of a number of elements, including:

- Raw water capture- involves the process of collecting raw water from a natural source, such as a river, lake or well. Raw water can be taken by various methods, such as surface abstraction, or through wells drilled into subsurface layers.

- Stage I pumping (if applicable): If the raw water source is at a lower level than the treatment plant or distribution network, a pumping station may be required to raise the water to the desired level.

- Supply pipes: these are pipes through which raw water is transported from the source to the treatment plant. The supply pipes are designed to ensure a continuous and efficient flow of water.

- Water treatment plant: this is a specialized installation, where raw water is treated and corrected, depending on the quality imposed on the consumer. The treatment processes can include sedimentation, filtration, disinfection operations to ensure the quality of drinking water.

The analyses to determine the values of the physico-chemical and bacteriological indicators of the water are carried out by the Drinking Water Laboratory, within the Quality Laboratory Service of the company, a laboratory that is registered with the Ministry of Health, in the Laboratory Register, which performs quality control monitoring drinking water.

- Reservoirs: these are constructions or containers, used to store the volume of water required for various purposes. The tanks provide a water reserve for emergency situations, to compensate for hourly consumption and to ensure the water required for firefighting.

- Second-stage pumping station (if applicable): If the water pressure in the distribution network is not sufficient, an additional pumping station may be required to ensure the necessary pressure in the network. In some cases, the pressure can be ensured by gravity, without the need for additional pumping stations.

- Distribution network: This consists of an extensive system of pipes and branches, which carry treated water from the treatment plant to consumers such as households, public or industrial buildings. The distribution network is designed to ensure the supply of drinking water, at the appropriate pressure and in sufficient quantity, at all points of consumption [7].

2. Simulation of fluid flow through pipes

When water moves along a pipe, the density differences can cause two phases to be distributed, in several different configurations, which can affect the operating conditions, for example: the angle of the

THE ANNALS OF "DUNAREA DE JOS" UNIVERSITY OF GALATI
FASCICLE IX. METALLURGY AND MATERIALS SCIENCE
N°. 2 - 2024, ISSN 2668-4748; e-ISSN 2668-4756
Article DOI: https://doi.org/10.35219/mms.2024.2.06

pipe, and the phase velocities, which determine the distribution phases in pipelines.

A flow that is unstable and complicated, can cause damage to the pipes, but also to the circuit, due to the speed of the liquid flow.

More or less deposits can remain on the pipes, which can lead to the appearance of extreme variation over time in the cross-sections of the pipes. Phase differences, and pressure, as well as flow rates, lead to destabilization of mass transfer processes [1, 3].

At the same time, flow interruptions can cause vibrations and pressure drops, along the entire length of the pipe, causing damage to the pipe supports, as well as corrosion of the pipes, in the lower part.

The simulation of flow in pipes or rings is very important, and has wide applicability in various industries, such as chemical processes, and petroleum industries, pipeline engineering, power plants, biomedical engineering. Simulation applications are also used in engineering, micro-scale fluid dynamics studies, in food processing industries, in geothermal flows and in the extrusion of molten plastic materials.

These simulations are also used in sludge flow (water-solid) and sludge flow (water-air), with applications in various industries, aiming to reduce environmental pollution.

This type of multiphase flow occurs frequently in horizontal pipes and channels.

The liquid-solid simulation has found its applicability to slurry flows, the transport of raw materials, waste and sludge, which are in solid form, their valorisation, and in extractive metallurgy and mining factories, coal processing plants, fluidized beds, oil industries and many more [2].

The sludge transport system helps to reduce air pollution, noise, save energy consumption, and better protection from an ecological point of view.

Computational fluid dynamics (CFD) is a programming and calculation method applied to study the behavior of two-phase flows.

The modeling of two-phase flows is time-consuming and very difficult, due to the involvement of advanced physics and mathematical calculations.

The flow simulation was carried out with the help of the SolidWorks program.

SolidWorks is a computer-aided design (CAD) software used primarily in the field of engineering and industrial design. This software is known for its advanced 3D modeling and simulation features.

The program helps us to create and use three-dimensional models in the virtual environment. The program has a wide range of tools and functions. This gives us options for solid modeling, surface modeling, assembly, animation, simulation and automatic drawing generation.

It uses a feature-based approach to 3D modeling, allowing objects to be created and edited by adding, modifying, or removing specific features. This provides precise control over the geometry.

With the help of integrated simulation functions, it allows testing and validation of models before manufacturing. The simulation program enables structural strength analysis, fluid flow simulations, thermal simulations and more. Simulations provide important information to optimize the design and identify potential problems, before production [4].

We used this program because it can simulate problems related to damage to equipment, installations and operational problems with equipment such as pipelines.

Phase distribution is a key component in the design of engineering structures due to its impact on various parameters such as flow load and pressure drop.

To study the flow mode, it is important to know both the system distribution and the flow regime under different boundary conditions.

The deposits during the flow move at a higher speed than the liquid, and can initiate strong vibrations, causing equipment damage.

Deposition frequency, which is defined as the number of coalesced particles that flow over a given point in a pipeline in a given period of time, is an important factor in determining operational capacity.

The program can simulate difficulties such as pipeline vibration and instability, wellhead pressure fluctuations, and flooding of downstream facilities. High frequency of deposits can cause pipe corrosion [5].

If the concentration of pipe vibrations is high, it can be caused by an unstable flow regime, changes in flow direction, or inadequate pipe diameter.

Severe pipe vibrations can affect their operation, and this can lead to unsafe and even dangerous conditions. Until now, the studies have mainly referred to the vibration of pipes due to mechanical causes, as sources of vibrations and not deposits.

The cause of fluid vibrations in pipelines has been studied using various theoretical methods.

The first stage of the simulation consisted in the creation of the object to be tested and analysed, namely the pipe (Fig. 1).

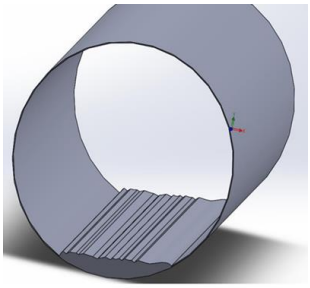

Fig. 1. *Pipe with the waste*

THE ANNALS OF "DUNAREA DE JOS" UNIVERSITY OF GALATI
FASCICLE IX. METALLURGY AND MATERIALS SCIENCE
Nº. 2 - 2024, ISSN 2668-4748; e-ISSN 2668-4756
Article DOI: https://doi.org/10.35219/mms.2024.2.06

For the simulation, we made a pipe with a diameter similar to that of the domestic water installation.

At the bottom of the image, depositions were simulated. I watched the impact of oxide deposits, from the lower part of the pipes.

The second part of the simulation consists in presenting the variation of the velocity of a fluid, in a parallel plane, which almost reaches the maximum diameter. The program shows us a maximum speed of 9m/s in the middle part of the pipe, where the fluid passes. Towards the side walls of the pipe, the maximum velocity of the fluid is approximately 4 m/s (Fig. 2).

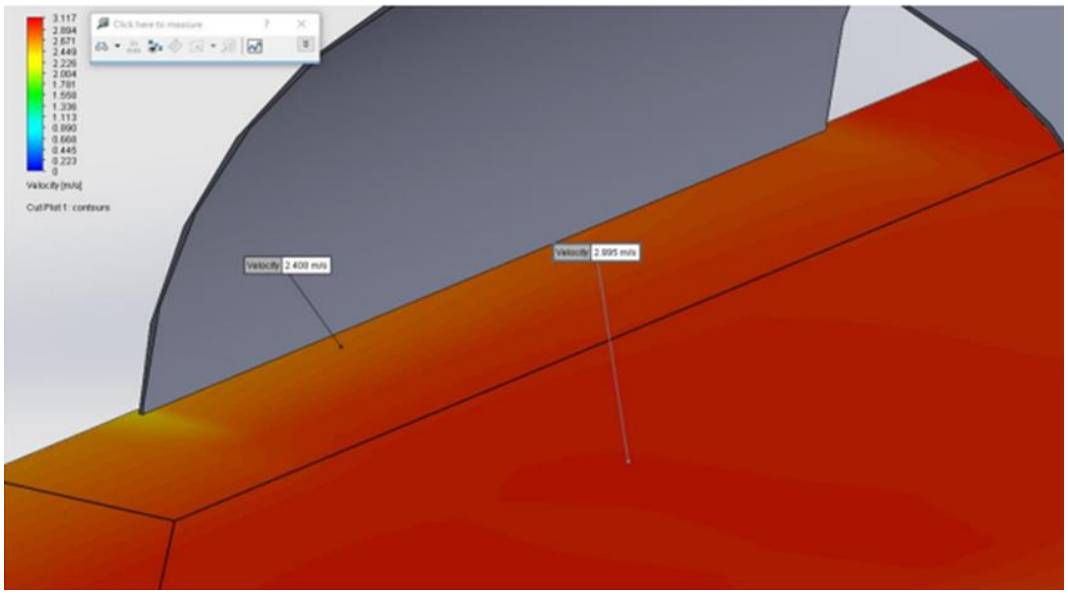

Fig. 2. *Variation of fluid velocity in a pipe*

At the bottom of the pipe, where the deposits are located, a very large decrease in the flow velocity can be observed, which can reach up to 0.8 m/s. In this case, the pressure will be higher, which will facilitate the transport of deposits from the bottom, if they will have smaller dimensions [6].

In the captured images from the simulation program (Fig. 3), you can see the distribution of the speed of the fluid, in the time of simulation.

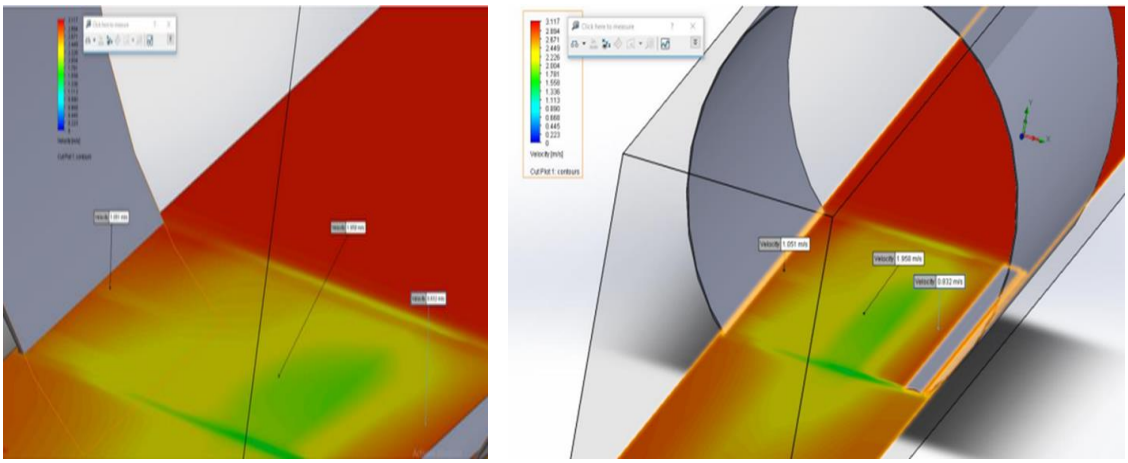

Fig. 3. *Fluid velocity distribution*

Following the simulations, it turned out that if the pressure drops to approximately 8 %, we will have a higher consumption for water transport in the network, due to the low pressure in the pipe (Fig. 4).

THE ANNALS OF "DUNAREA DE JOS" UNIVERSITY OF GALATI
FASCICLE IX. METALLURGY AND MATERIALS SCIENCE
No. 2 - 2024, ISSN 2668-4748; e-ISSN 2668-4756
Article DOI: https://doi.org/10.35219/mms.2024.2.06

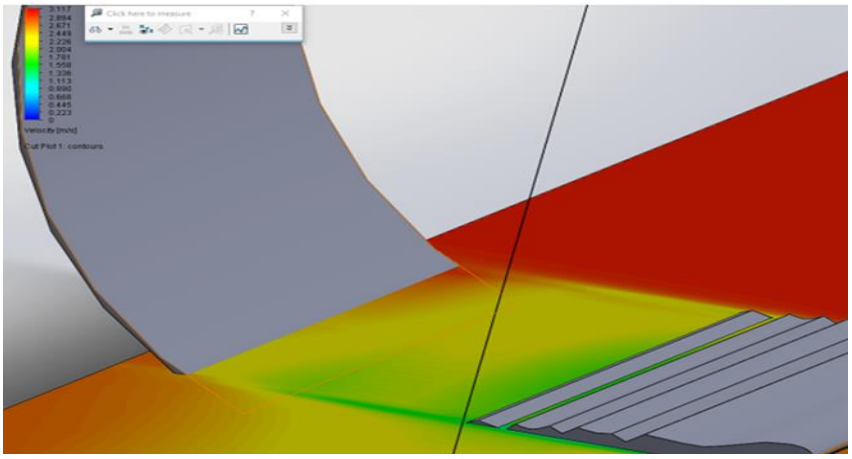

Fig. 4. *Low pressure in the pipeline*

3. Conclusions

The flow simulation was carried out with the help of the SolidWorks program.

The deposits during the flow move at a higher speed than the liquid, and can initiate strong vibrations, causing equipment damage.

The simulation consists in presenting the variation of the speed when a fluid flows, in a parallel plane, which reaches almost the maximum diameter.

Following the simulations, it turned out that if the pressure drops to approximately 8 %, a higher consumption will be induced for water transport, in the household water transport network.

References

[1]. Neamtu Catalin, Daniela Popescu, Bodi Stefan, Comes Radu, Curta Razvan, *SolidWorks 2016: Indrumator de laborator*, ISBN 978-606-543-906-1, Editura Mega, Cluj-Napoca, 2017.
[2]. Király Andrei, Bălcău Monica, *Grafică pe Calculator - SolidWorks – Îndrumător*, Editura MEGA, ISBN 978-606-543-141-6, Cluj-Napoca, 2011.
[3]. Jurco Ancuța-Nadia, *Noțiuni introductive în desenul tehnic industrial*, Editura UTPRESS, Cluj-Napoca, ISBN 978-606-737-617-3, https://biblioteca.utcluj.ro/files/carti-onlinecu-coperta/617-3%20.pdf, 2022.
[4]. Bodea Sanda, *Desen tehnic – Elemente de proiectare*, Editura RISOPRINT, ISBN 973-656-353-7, Cluj-Napoca, 2008.
[5]. Bodea Sanda, *Reprezentări grafice inginerești*, Editura RISOPRINT, ISBN 978-973-53-0144-6, Cluj-Napoca, 2010.
[6]. ***, *SolidWorks Online Help*, http://help.solidworks.com.
[7]. ***, https://www.apa-gaz-canalizare.ro/alimentare-cu-apa-potabila.

THE ANNALS OF "DUNAREA DE JOS" UNIVERSITY OF GALATI
FASCICLE IX. METALLURGY AND MATERIALS SCIENCE
N°. 2 - 2024, ISSN 2668-4748; e-ISSN 2668-4756
Article DOI: https://doi.org/10.35219/mms.2024.2.07

EXPERIMENTAL RESEARCH ON DETERMINING THE TRANSMITTANCE OF LENSES FOR VISION CORRECTION AND THE FACTORS THAT INFLUENCE IT

Beatrice Daniela TUDOR, Iustina BĂBUȘANU
"Dunarea de Jos" University of Galati, Romania
e-mail: beatrice.tudor@ugal.ro

ABSTRACT

The field of making optical lenses is very vast and with great applicability in several engineering fields. The research carried out in this work implied the determination of the transmittance of optical lenses of different diopters, thicknesses, with and without protection and the influence of material from which they were made. By analysing different aspects of lenses, we can better understand their impact on patients' vision and visual comfort, thus contributing to improving the quality of ophthalmic services.

KEYWORDS: transmittance, lenses, optical properties, diopters

1. Introduction

Optical lenses are essential components of many optical devices such as glasses, cameras, telescopes and microscopes. Lens manufacturing technology has developed significantly over the years, leading to improvements in precision, performance and cost.

Lenses can be made from a variety of materials, including glass, plastic, and crystal. Each material has specific optical and mechanical properties, which influence the performance and use of the lenses [1, 4].

Optical properties:

• Focusing: is their ability to focus light. Converging (convex) lenses focus parallel light to meet at a point called the focal point, while diverging (concave) lenses cause parallel light rays to spread out.

• Transmittance: refers to the proportion of light that passes through a lens and is transmitted into the optical system. A lens with a high transmittance allows more light to pass through, which can improve image clarity and brightness.

• Reflection: Lenses can suffer from unwanted reflections, which can affect the quality of images. Optical treatments, such as anti-reflective coatings, are used to reduce reflections and improve light transmission through the lens.

• Optical power: The power of a lens, is measured in diopters, and indicates the ability of the lens to focus light. Higher power lenses have a more pronounced curve, and can focus light to a smaller point.

• Aberration: Perfect lenses should focus all light rays to a single point. However, in practice, lenses can suffer from optical aberrations, which can include chromatic aberrations (differences in focus depending on colour), spherical aberrations (distortions of the image at the edge of the lens), and coma (deviations from actual focal points). The control and correction of aberrations are essential to ensure the quality of the images and the optical performance of the lenses.

• Light transmission: Lenses must be transparent to allow light to pass through with as little loss as possible. The materials used in the manufacture of lenses must be selected and processed so that they have a high optical transmission in the spectrum of interest.

• Dispersion: Dispersion refers to how the lens separates the different colours of light. Lenses with lower dispersion are preferred in many applications to minimize the effects of chromatic aberration.

• Distortions: Lenses can cause image distortions, such as pincushion or barrel distortion, which can affect the clarity and precision of images. Correcting these distortions is important in applications such as photography and medical imaging.

Transmittance is defined as the ability of a material to allow the passage of certain factors, such as light, heat or electrical signals, without significantly changing its properties. Transmittance is a measure of the degree to which a medium allows

THE ANNALS OF "DUNAREA DE JOS" UNIVERSITY OF GALATI
FASCICLE IX. METALLURGY AND MATERIALS SCIENCE
Nº. 2 - 2024, ISSN 2668-4748; e-ISSN 2668-4756
Article DOI: https://doi.org/10.35219/mms.2024.2.07

the flow or transfer of a certain characteristic or energy.

The transmittance of optical lenses refers to their ability to allow light to pass through a specific range of wavelengths. It is a measurement that tells us how much light is transmitted through the lens relative to how much is absorbed or reflected [2, 5].

The transmittance of optical lenses is influenced by:

1. Lens material: The materials used to make lenses have different optical properties. For example, glass, crystal and plastic have different optical transmittances, influenced by their molecular structure and possible impurities.

2. Lens thickness: Lens thickness can affect transmittance because some of the light can be absorbed into the lens material as it passes through it. Thicker lenses can absorb more light than thinner ones.

3. Anti-reflective coatings: Optical lenses can be coated with thin layers of materials to reduce unwanted reflections and increase transmittance. These anti-reflective coatings are designed to minimize light loss through reflection and improve lens performance.

4. Adjusting lenses with special applications: In some cases, lenses can be dissolved in certain solutions to improve transmittance, particularly in special applications or in the case of very thick lenses.

5. Optical design: Lens geometry and design can also affect transmittance. For example, lenses with less curved surfaces or manufacturing defects may have lower transmittance.

The transmittance of optical lenses is important in many applications, such as: medical optics, imaging equipment and measuring instruments. In these applications it is important to minimize light losses to obtain accurate and clear results [2, 3].

2. Research on determining the transmittance of lenses for vision correction

The research on determining the transmittance was carried out on a group of lenses of different thicknesses and diopters.

The transmittance tests were done on five lenses:

- Diopter -0.50 medium protection lenses with 1.25 mm lens thickness.
- Diopter -0.50 lenses without protection with a lens thickness of 1.20 mm.
- Diopter -0.25 medium protection lenses with 1.17 mm lens thickness.
- Diopter -0.25 lenses without protection with a lens thickness of 1.15 mm.
- Diopter -5 medium protection lens with 2.30 mm lens thickness.

The transmittance of the lenses was performed on the HACH LANGE DR5000 device with a gas-filled Tungsten lamp and a deuterium (UV) lamp and with a wavelength range between 190-1100 nm (Fig. 1).

Fig. 1. *HACH LANGE DR5000 device for determining transmittance*

The stages of making the measurements are:

- measuring the thickness of the lens (Fig. 2);
- placing the lens in the device;
- blocking the device for generating determinations;
- generating graphs for transmittance (Fig. 3);
- data transfer to a stick.

Fig. 2. *Measuring lens thickness*

The data obtained on the HACH LANGE DR5000 device for the determination of transmittance are partially presented in Table 1.

After centralizing the data in the table, we obtained the following spectra for the transmittance of the lenses shown in Fig. 4, 5.

For lenses with medium protection, we obtained a higher transmittance than the ones with -0.25 and 1.17 mm thickness because the lower thickness allows a greater flow of light to pass through.

THE ANNALS OF "DUNAREA DE JOS" UNIVERSITY OF GALATI
FASCICLE IX. METALLURGY AND MATERIALS SCIENCE
N°. 2 - 2024, ISSN 2668-4748; e-ISSN 2668-4756
Article DOI: https://doi.org/10.35219/mms.2024.2.07

In the unprotected lenses we obtained a higher transmittance at the -0.50 diopter lens, because it had a higher lens power, measured at one meter focal length than the -0.25 diopter lens.

We have noticed that in lenses without protection, the transmittance is less influenced by the thickness of the lens, a stronger influence of the transmittance being given by its diopter.

The comparison of transmittance spectra for both lens categories is shown in the graph in Fig. 6.

By comparing the transmittance spectra, we found that the lens thickness had the greatest influence on lenses with medium protection. At the lens taken in the study with the largest thickness, namely 2.30 mm (the -5 diopter lens), we obtained the lowest transmittance.

Fig. 3. *Generating graphs*

Table 1. *Data obtained for lens transmittance*

Wavelength	-0.50 medium protection lens	-0.50 lens without protection	-0.25 medium protection lens	-0.25 lens without protection	Medium protection - 5 lens
190	0.189	0.177	0.158	0.144	0.115
191	0.138	0.136	0.114	0.101	0.089
192	0.122	0.118	0.1	0.09	0.076
193	0.107	0.097	0.092	0.074	0.076
194	0.094	0.094	0.072	0.074	0.057
195	0.084	0.079	0.067	0.06	0.064
196	0.078	0.075	0.062	0.06	0.05
197	0.061	0.064	0.052	0.051	0.021
198	0.047	0.049	0.047	0.029	0.022
199	0.052	0.051	0.033	0.025	0.028
200	0.053	0.043	0.038	0.027	0.029
201	0.054	0.045	0.038	0.022	0.02
202	0.042	0.041	0.031	0.029	0.023
203	0.042	0.04	0.03	0.029	0.019
204	0.036	0.036	0.033	0.023	0.032
205	0.039	0.034	0.029	0.024	0.018
206	0.034	0.04	0.03	0.022	0.02
207	0.036	0.038	0.035	0.025	0.018
208	0.04	0.04	0.029	0.023	0.015

THE ANNALS OF "DUNAREA DE JOS" UNIVERSITY OF GALATI
FASCICLE IX. METALLURGY AND MATERIALS SCIENCE
N°. 2 - 2024, ISSN 2668-4748; e-ISSN 2668-4756
Article DOI: https://doi.org/10.35219/mms.2024.2.07

209	0.035	0.035	0.025	0.018	0.018
210	0.034	0.37	0.029	0.021	0.012
211	0.033	0.03	0.025	0.021	0.02
212	0.031	0.034	0.023	0.026	0.016
213	0.035	0.033	0.024	0.023	0.023
214	0.038	0.027	0.024	0.024	0.016
215	0.036	0.03	0.026	0.024	0.01
216	0.034	0.027	0.024	0.021	0.016
217	0.033	0.027	0.025	0.021	0.015
218	0.036	0.035	0.028	0.023	0.016
219	0.029	0.027	0.027	0.024	0.018
220	0.037	0.031	0.025	0.023	0.014
221	0.031	0.03	0.024	0.023	0.02
222	0.033	0.03	0.023	0.025	0.016
223	0.04	0.031	0.023	0.023	0.015
224	0.03	0.029	0.024	0.015	0.016
225	0.037	0.034	0.025	0.02	0.017
226	0.031	0.032	0.02	0.021	0.022
227	0.032	0.034	0.02	0.016	0.02
228	0.035	0.028	0.018	0.029	0.014
229	0.034	0.027	0.024	0.019	0.017
230	0.033	0.028	0.022	0.019	0.017

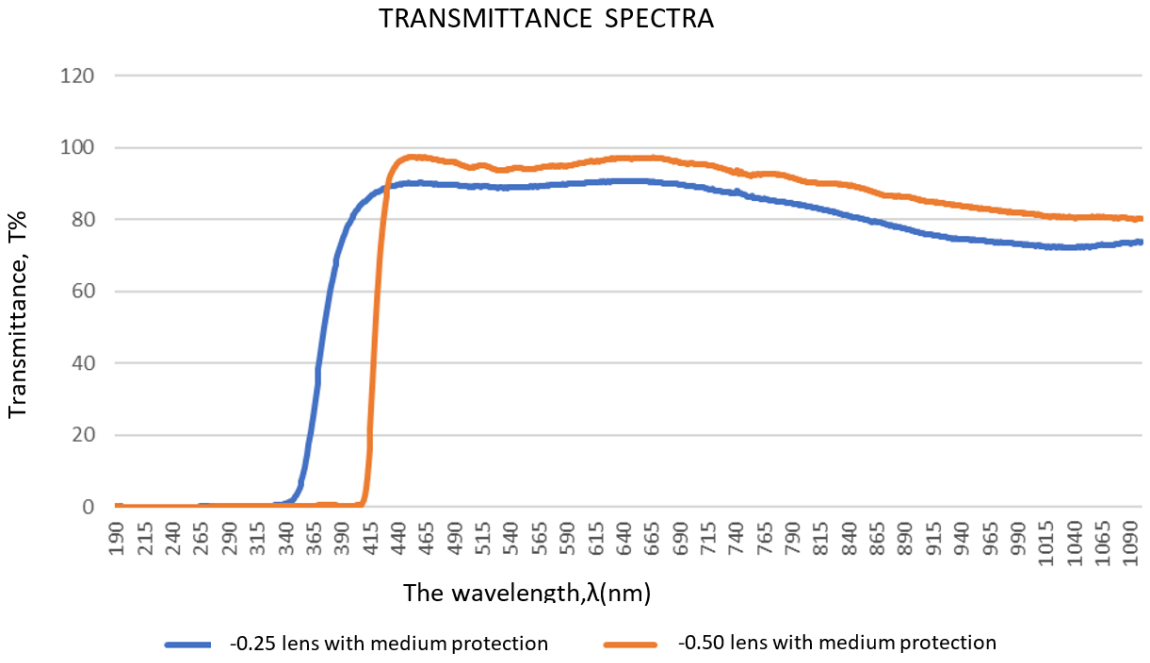

Fig. 4. *Transmittance spectrum of medium protection lenses*

THE ANNALS OF "DUNAREA DE JOS" UNIVERSITY OF GALATI
FASCICLE IX. METALLURGY AND MATERIALS SCIENCE
Nº. 2 - 2024, ISSN 2668-4748; e-ISSN 2668-4756
Article DOI: https://doi.org/10.35219/mms.2024.2.07

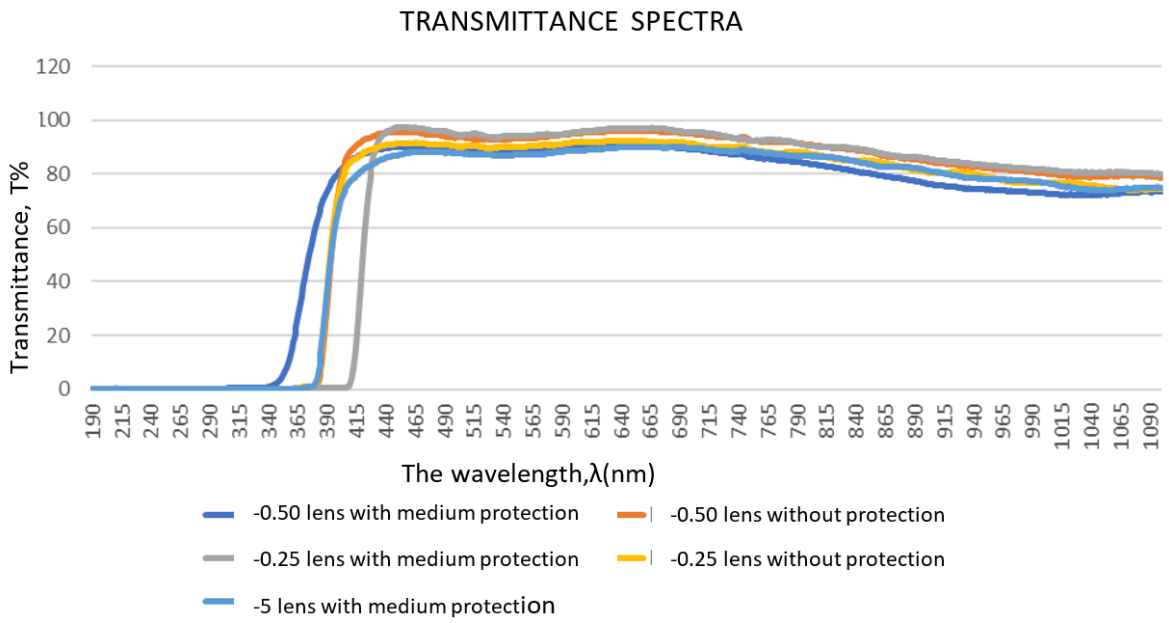

Fig. 5. *Transmittance spectrum for lenses without protection*

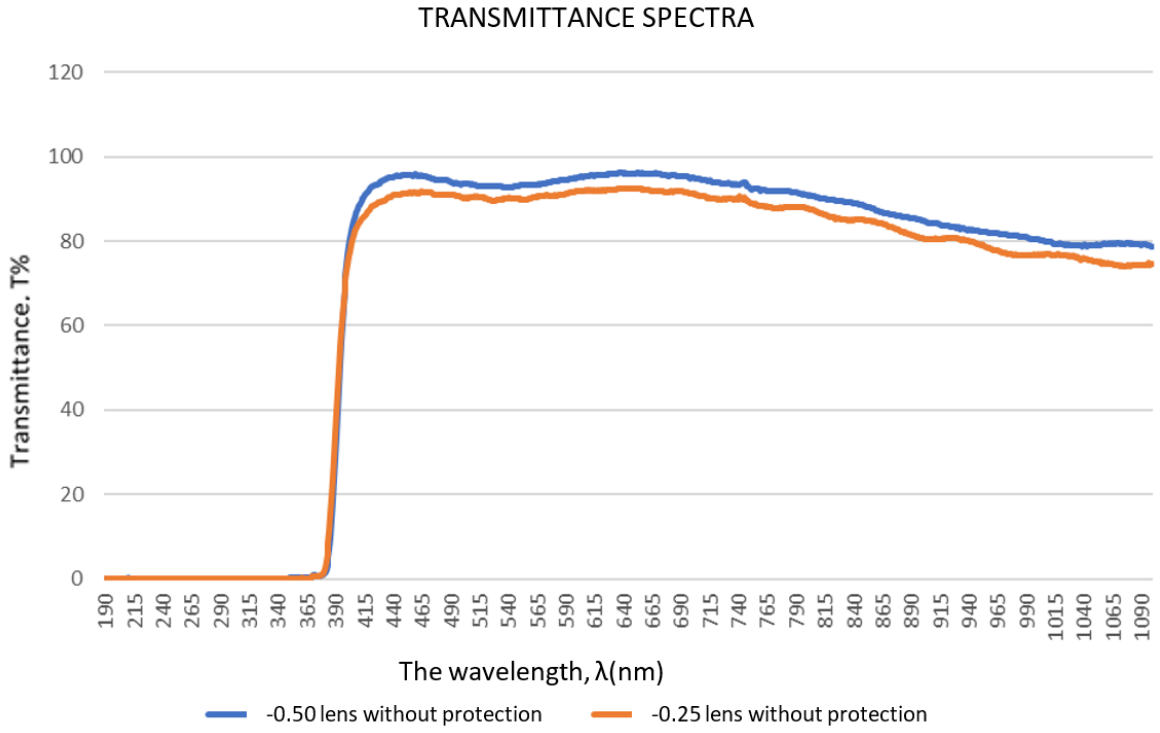

Fig. 6. *Comparison of the transmittance spectra of the both lens categories*

3. Conclusions

After the determinations made, we came to the conclusion that the transmittance of the lenses was influenced by several factors, respectively: diopters, the thickness of the lens, the protection applied to them and the material from which they were made.

At medium protection lenses with diopters of -0.50 and thickness of 1.25 mm, transmittance values were lower compared to medium protection lenses

THE ANNALS OF "DUNAREA DE JOS" UNIVERSITY OF GALATI
FASCICLE IX. METALLURGY AND MATERIALS SCIENCE
N°. 2 - 2024, ISSN 2668-4748; e-ISSN 2668-4756
Article DOI: https://doi.org/10.35219/mms.2024.2.07

with -0.25 diopters and 1.17 mm thickness, as lens thickness influenced lens transmittance. The lowest transmittance in lenses with medium protection has been obtained in the lens with the largest thickness respectively 2.30 mm and with diopter of -5.

In the case of unprotected lenses, transmittance values were higher for lenses with -0.50 diopters compared to those with -0.25 diopters. For this type of lens, the greatest influence on the transmittance is the diopter value and not the lens thickness.

At the medium protection -5 diopter lens with 2.30 mm lens thickness, we got a lower transmittance which meant that if the diopters were very large, the lens thickness would negatively influence the transmittance.

From the point of view of the material from which the lenses are made, the PMMA polymethacrylate methacrylate lens (the -5 diopter lens) transmittance was lower than the organic glass lenses (the -0.50 and -0.50 diopter lenses -0.25).

By analysing different aspects of lenses, we can better understand their impact on patients' vision and visual comfort, thus contributing to improving the quality of ophthalmic services.

References

[1]. Cristea Dumitru, *'Sisteme anatomice ale organismului uman*, Editura Academica, Galați, p. 40-65, 2001.
[2]. Olteanu M., *Tratat de oftalmologie*, vol. I and II, Editura Medicală, București, p. 36-70, 1989.
[3]. ***, https://www.everydayhealth.com/vision/new-directions-whats-coming-down-the-pike-in-eyewear.
[4]. ***, www.icf.ro/Institut/lab04/XPS_ESCA_book2009.pdf.
[5]. ***, https://www.agir.ro/buletine/410.pdf.
[6]. ***, https://infosan.ro/anatomia-ochiului-secrete-si-curiozitati-fascinante-despre-sistemul-ocular/.

MANUSCRISELE, CĂRŢILE ŞI REVISTELE PENTRU SCHIMB, PRECUM ŞI ORICE CORESPONDENŢE SE VOR TRIMITE PE ADRESA:

MANUSCRIPTS, REVIEWS AND BOOKS FOR EXCHANGE COOPERATION, AS WELL AS ANY CORRESPONDANCE WILL BE MAILED TO:

LES MANUSCRIPTS, LES REVUES ET LES LIVRES POUR L'ECHANGE, TOUT AUSSI QUE LA CORRESPONDANCE SERONT ENVOYES A L'ADRESSE:

MANUSCKRIPTEN, ZIETSCHRITFTEN UND BUCHER FUR AUSTAUCH SOWIE DIE KORRESPONDENZ SID AN FOLGENDE ANSCHRIFT ZU SEDEN:

After the latest evaluation of the journals by the National Center for Science Policy and Scientometrics (**CENAPOSS**), in recognition of its quality and impact at national level, the journal will be included in the B^+ category, 215 code (http://cncsis.gov.ro/userfiles/file/CENAPOSS/Bplus_2011.pdf).

The journal is already indexed in:
DOAJ: https://doaj.org/
SCIPIO-RO: http://www.scipio.ro/web/182206
EBSCO: http://www.ebscohost.com/titleLists/a9h-journals.pdf
Google Academic: https://scholar.google.ro
Index Copernicus: https://journals.indexcopernicus.com
Crossref: https://search.crossref.org/

The papers published in this journal can be viewed on the website: http://www.gup.ugal.ro/ugaljournals/index.php/mms

Name and Address of Publisher:
Contact person: Prof. Dr. Eng. Elena MEREUȚĂ
Galati University Press - GUP
47 Domneasca St., 800008 - Galati, Romania
Phone: +40 336 130139
Fax: +40 236 461353
Email: gup@ugal.ro

Name and Address of Editor:
Ș. L. Dr. Eng. Marius BODOR
"Dunarea de Jos" University of Galati, Faculty of Engineering
111 Domneasca St., 800201 - Galati, Romania
Phone: +40 336 130208
Phone/Fax: +40 336 130283
Email: marius.bodor@ugal.ro

AFFILIATED WITH:

- THE ROMANIAN SOCIETY FOR METALLURGY
- THE ROMANIAN SOCIETY FOR CHEMISTRY
- THE ROMANIAN SOCIETY FOR BIOMATERIALS
- THE ROMANIAN TECHNICAL FOUNDRY SOCIETY
- THE MATERIALS INFORMATION SOCIETY (ASM INTERNATIONAL)

Edited under the care of the FACULTY OF ENGINEERING

Annual subscription (4 issues per year)

Fascicle DOI: https://doi.org/10.35219/mms

Volume DOI: https://doi.org/10.35219/mms.2024.2

Editing date: 15.06.2024
Number of issues: 200
Printed by Galati University Press (accredited by CNCSIS)
47 Domneasca Street, 800008, Galati, Romania